

APPENDIX VII

MATES III

DRAFT FINAL REPORT

**PM_{2.5} Source Apportionment for the South Coast Air Basin Using
Chemical Mass Balance Receptor Model**

Authors

Tuyet-Le Pham
Bong-Mann Kim
Aaron Katzenstein
Tracy Goss

Appendix VII

PM_{2.5} Source Apportionment for the South Coast Air Basin Using Chemical Mass Balance Receptor Model

VII-1 Introduction

The MATES II Study found that the major contributor to risk from ambient air toxics was diesel exhaust. Since there is no method to directly measure diesel particulate matter, an indirect method must be used. In MATES II, the concentration of elemental carbon (EC) in PM₁₀ filter samples was multiplied by a factor of 1.04 to estimate diesel particulate matter for cancer risk assessment. The presence of high levels of EC within diesel exhaust is a unique property of this combustion source. A factor of 1.04 was determined from diesel source profiles and fine particle samples collected in 1982. Due to uncertainty from this approach, the MATES III Technical Review Group recommended using speciated analysis conducted upon the collected PM_{2.5} filters within a Chemical Mass Balance (CMB) model to estimate diesel contributions. The Positive Matrix Factorization (PMF) receptor model was also suggested.

PM_{2.5} source apportionment for the Basin was conducted using the CMB receptor model 8.2 approved by the U.S. EPA and the MATES III ambient data collected over a two-year period from March 2004 to April 2006 at the ten MATES III monitoring stations.

In particular, gasoline and diesel-vehicle contributions were differentiated with the use of organic compounds (Chow et al. 2007). Contributions of other primary sources to ambient PM_{2.5} mass concentrations (biomass burning, cooking operations, sea salt, geological, residual oil burning, and limestone) were also estimated.

VII-2 MATES III SOURCE APPORTIONMENT

CMB Model

The CMB model was first developed by Miller, et al. (1972) and further refined by Friedlander (1973) and Watson (1979). The CMB model, which uses selected chemical species as mass balance fitting species, is a tool to estimate source contributions. The ambient concentration of chemical species i is expressed as a linear equation:

$$C_i = \sum_{j=1}^p a_{ij} S_j, i=1,n$$

where a_{ij} is fractional concentration of chemical species i in source j , S_j is total mass concentration contributed by source j , p is number of sources, and n is number of species.

Since the number of chemical species, n , is usually larger than the number of sources, p , the system is over-determined and the least-squares fitting approach is applied. The model requires the identification of emission sources, the selection of chemical species and source profiles, and the

ambient data. Input uncertainty is critical to the model since it determines the importance of input data to the model solutions (EPA, 2004). In summary, the CMB source apportionment is depicted by the following flowchart:

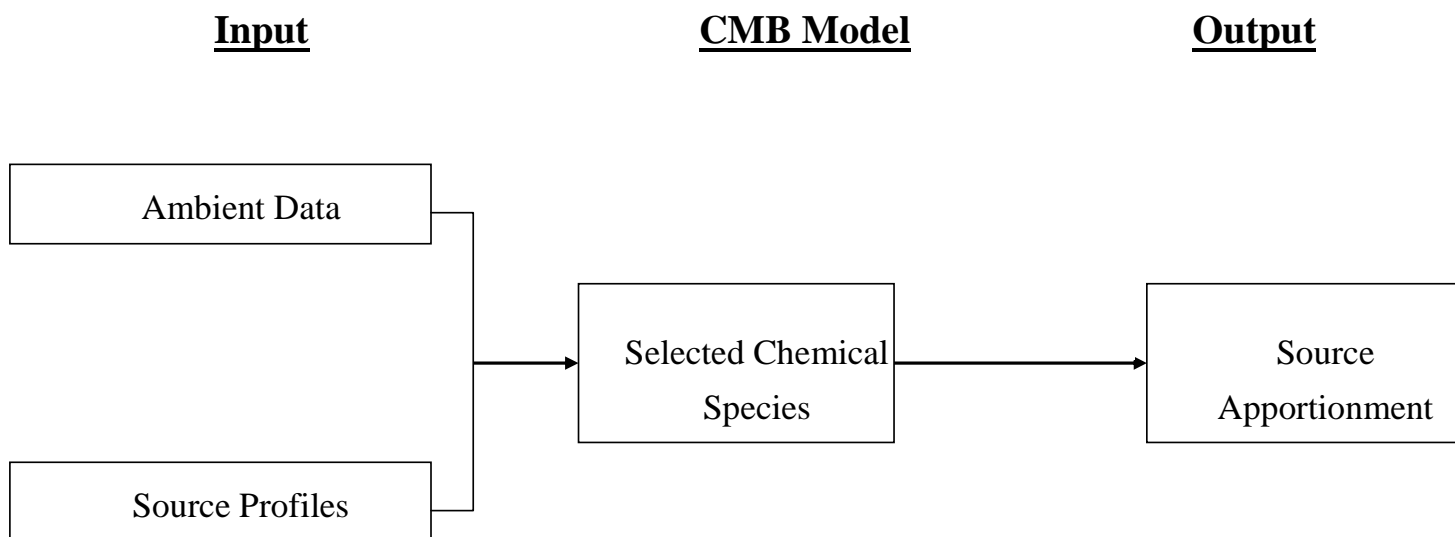


Figure 1. Source Apportionment Flowchart

MATES III Ambient Data

Monthly-averaged ambient data from samples collected at the ten fixed MATES III sites [West Long Beach (WLB), North Long Beach (NLB), Compton (CP), Huntington Park (HP), Pico Rivera (PR), Los Angeles (LA), Burbank (BU), Inland Valley/San Bernardino (SB), Rubidoux (RU), and Anaheim (AN)] were utilized. Sampling was conducted every three days over a two-year period from March 2004 to April 2006. Since October 2004 through February 2005 was not considered a typical winter season for the Basin (with 56 rainy days and 24.2 to 33.9 inches of rain in Los Angeles and Long Beach per National Climatic Data Center), MATES III sampling program was extended one more year to April 2006. During the second year (2005-2006), sampling was not conducted in Pico Rivera and Huntington Park for a full year. Elemental Carbon (EC), organic carbon (OC), ions, metals, and monthly-composite organics samples were analyzed. Details of the sites and sampling protocols are given in Chapter 2.

Selected Source Profiles

Before selecting the source profiles, available and pertinent previous studies were reviewed. Great care was made to ensure that the chosen source profiles represented the Basin and therefore were most applicable for this study. The following source profiles for the MATES III source apportionment model and their basis for selection are as follows:

- *Ammonium Nitrate and Ammonium Sulfate Profiles*

Single constituent source profiles consisting of pure nitrate and sulfate (Chow, et al. 2007) were used.

- *Biomass Burning Profile*

A biomass burning profile was developed for the Basin by Schauer (1998) based on the testing of residential fireplaces burning oak wood. This profile was selected due to the similarity of its levoglucosan (0.138 ± 0.0001) mass fraction compared to the levoglucosan level from the most recent and comprehensive combined profile developed by Fine (2002) for fireplace and woodstove combustion (0.126 ± 0.0002). In these profiles, OC, EC, and TC (total carbon) were analyzed accordingly to the NIOSH protocol that was different than the IMPROVE thermal/optical reflectance (TOR) protocol used in the MATES III.

In addition, another biomass burning profile developed by Desert Research Institute (DRI) for use in a source apportionment study in Fresno (Chow, et al. 2007) was also applied to the Los Angeles, West Long Beach, and Rubidoux CMB source apportionment for comparison purposes.

- *Cooking Profile*

A meat cooking profile consisting of average data from charbroiling chicken with skin on was developed by Zielinska, et al. (1998). This profile applied the same IMPROVE TOR protocol that was used in the MATES III to analyze OC, EC, and TC.

- *Diesel Exhaust Profile*

A diesel motor-vehicle profile was developed during the summer of 2001 for the Basin as part of the Department of Energy's (DOE) Gasoline/Diesel PM Split Study (Fujita, et al. 2006) and was normalized to $PM_{2.5}$ mass for use in the Fresno Supersite study (Chow, et al. 2007). This profile was selected because: (1) it was the most recently developed and comprehensive one that tested 34 diesel vehicles of various vehicle weights and model years operated under various cycles; (2) it was the profile where OC, EC, and TC were analyzed using the same IMPROVE TOR protocol that was applied in MATES III; (3) it was also used in the most recent CMB studies (Chow, et al. 2007 and Lough, et al. 2005); and (4) it generated better model performance statistics that are more acceptable to the CMB practice.

However, sensitivity tests for mobile diesel exhaust have also been conducted for Los Angeles. In particular, various diesel profiles from the Northern Front Range Air Quality Study (NFRAQS) were applied. The poor performance statistics indicate that these diesel profiles were not adequate for the model.

- *Gasoline-Vehicle Exhaust Profile*

A gasoline motor-vehicle profile developed for the Basin as part of the DOE's Gasoline/Diesel Split Study (Fujita, et al. 2006) and normalized to $PM_{2.5}$ mass for use in the Fresno Supersite study (Chow, et al. 2007) was selected. This profile was based on the testing of 57 gasoline vehicles of various model years and mileages operated under various cycles.

In addition, another profile (Zielinska, et al. 1998) developed during summer 1996 and winter 1997 for the NFRAQS was also selected. This profile was based on the testing of a larger fleet consisting of 111 gasoline vehicles under various operating cycles and also utilized the same IMPROVE TOR protocol used in the MATES III to analyze EC, OC, and TC. Since

mobile source emissions vary upon ambient temperature (Mathis, et al. 2005), fuel use, engines, driving modes, and lubricating oil (Lough and Schauer, 2005); the differences in fleet composition and ambient temperature were recognized. Therefore, both gasoline profiles were utilized for the analysis and a range for gasoline motor exhaust contribution was provided.

- *Sea Salt Profile*

An “aged” sea salt profile was developed by Chow, et al. (1996), which reflects a reaction of sea salt and nitric acid (HNO₃) where 0.5 mole of chlorine (Cl⁻) was replaced by one mole of nitrate (NO₃⁻).

- *Geological Profile*

A geological profile was developed by Chow, et al. (2003) from paved road suspended dust samples collected in the San Joaquin Valley. Although this profile was not developed for the Basin, its mass fractions (0.052 ± 0.01) of iron (Fe) and (0.035 ± 0.01) of calcium (Ca) are similar to those in Cooper, et al.’s profile (1987) developed for the Basin (0.052 ± 0.02 for Fe) and (0.035 ± 0.01 for Ca). Fe and Ca were two of the three selected fitting species for geological apportionment in the MATES III CMB.

- *Residual Oil Burning Profile*

A residual oil burning profile was developed for the Basin by AQMD (1989) based on samples collected from a residual oil-fired boiler at a power plant in the Basin. Residual oil burning is mainly used in ships (Corbett and Fischbeck, 1997). Although vanadium (V) and nickel (Ni) concentration in residual oil is minimal compared to that of sulfur, vanadium is a unique species to characterize ship PM emissions.

- *Limestone Profile*

A profile developed by AQMD (1989) from the testing of Portland cement in a kiln was used only for the Rubidoux site.

Selected Fitting Species

Fitting species were pre-selected based on information from previous studies and further screened based on their correlation co-efficients and ambient concentrations. Species with higher ambient concentrations than their uncertainties and species with high correlation co-efficients (correlation co-efficients ≥ 0.8) were selected. However, the ambient concentration criteria was not strictly applied to levoglucosan, cholesterol, palmitoleic acid, coronene, indeno [123-cd]pyrene, and benzo(ghi) perylene, which often have low ambient concentrations.

The following were selected fitting species for the MATES III source apportionment categorized by their major sources:

- Ammonium nitrate and ammonium sulfate: NO₃⁻ and SO₄⁻²
- Biomass burning: Levoglucosan and potassium (K)
- Meat cooking: Cholesterol and palmitoleic acid

- Diesel-vehicle exhaust: EC, Steranes 48 and 49, Hopanes 17, 19, 24, and 26
- Gasoline-vehicle exhaust:
 - Indeno[123-cd]pyrene, benzo(ghi)perylene, coronene
 - Steranes 48 and 49
 - Hopanes 17,19, 24, and 26
- Sea salt: sodium (Na^+) and chlorine (Cl^-)
- Geological: Silica (Si), calcium (Ca), and iron (Fe)
- Residual oil burning: Vanadium (V) and nickel (Ni)

Organic carbon (OC) was not used in the CMB analysis because measured ambient OC is believed to be biased high. The flow rate (6.7 lpm) of the SASS PM sampler used during MATES III was approximately three times slower than that (20 lpm) of the Multi-Channel Fine Particulate (MCFP) sampling system used for the measurements of EC, OC, ions, and trace metals as part of the PTEP (1995) and MATES II studies. Higher flow rate is believed to have a greater stripping effect upon lighter organic compounds that may accumulate during slower flow. Slower flow rate in the SASS sampler reduces pressure drop through the sampler and increases the absorption of lighter organic compounds on quartz filter medium. Therefore, OC measured by the SASS sampler is often higher than that measured by the higher flow MCFP sampler. This positive OC bias leads to a higher total carbon (TC) than total mass due to the deposition difference between the quartz filters that were used to collect EC, OC, TC and Teflon filters that were used for mass (Turpin, et al. 1994). While $\text{PM}_{2.5}$ mass decreased 20 – 40% in 2004 compared to the 1995 ambient data, EC decreased 50 – 57%, nitrate decreased 30 – 54%, and sulfate decreased 11-25%, only organic carbon increased 13 to 50%. Additionally, the SASS sampler did not account for positive OC artifacts by using backup filters.

VII-3 Results and Discussion

The $\text{PM}_{2.5}$ source apportionment was conducted independently for each sampling year, using the same source profiles and fitting species. Specifically, the monthly source apportionment for the fixed sites was conducted by targeting R^2 values of 0.8 to 1.0, Chi^2 values of less than 4.0, and differences between calculated and measured $\text{PM}_{2.5}$ mass of less than 20%, which are the CMB optimal performance criteria.

The modified pseudo-inverse matrix (MPIN) diagnostic, an option to identify influential chemical species (Kim and Henry, 1989) shows that EC (with normalized MPIN absolute value of 1.0) is the most influential chemical species for diesel-vehicle exhaust, while the three PAHs (with absolute values ≥ 0.5): indeno [123-cd]pyrene, benzo(ghi) perylene, and coronene found in used gasoline motor oil, and sterane 48 found in engine lubricating oil (Fujita, et al. 2006) are most influential species to gasoline-vehicle exhaust in this model.

April 2004 – March 2005 (First-Year) PM_{2.5} Source Apportionment

Both Basin and the NFRAQS gasoline profiles were used in two CMB estimates, holding all other source profiles the same.

With the Basin Gasoline Profile

A Basin gasoline-vehicle profile used in the Fresno Supersite Study (Chow, et al. 2007) was applied to the CMB analysis.

The annual-average source contribution estimates of major PM_{2.5} source categories (in $\mu\text{g}/\text{m}^3$) and their percentages of the total predicted mass are summarized in Table 1 and Figure 2.

Table VII-1
First-Year PM_{2.5} Source Contribution Estimates - Basin Gasoline Profile

	WLB	NLB	CP	HP	PR	LA	BU	SB	RU	AN	10-Site Ave.
Ammonium Nitrate	4.39 <i>(22.0)</i>	5.14 <i>(27.2)</i>	5.68 <i>(27.3)</i>	6.99 <i>(30.5)</i>	7.03 <i>(32.8)</i>	7.04 <i>(34.0)</i>	7.33 <i>(35.0)</i>	8.42 <i>(37.7)</i>	10.08 <i>(44.8)</i>	5.70 <i>(32.3)</i>	6.78 <i>(31.6)</i>
Ammonium Sulfate	5.68 <i>(28.5)</i>	5.68 <i>(30.0)</i>	5.43 <i>(26.1)</i>	5.68 <i>(24.8)</i>	5.22 <i>(24.4)</i>	5.06 <i>(24.4)</i>	4.75 <i>(22.7)</i>	4.53 <i>(20.3)</i>	4.49 <i>(19.9)</i>	4.81 <i>(27.3)</i>	5.13 <i>(23.9)</i>
Biomass Burning	0.57 <i>(2.8)</i>	0.28 <i>(1.5)</i>	0.20 <i>(1.0)</i>	0.15 <i>(0.7)</i>	0.34 <i>(1.6)</i>	0.28 <i>(1.3)</i>	0.33 <i>(1.6)</i>	0.22 <i>(1.0)</i>	0.38 <i>(1.7)</i>	0.22 <i>(1.3)</i>	0.30 <i>(1.4)</i>
Cooking	1.93 <i>(9.6)</i>	1.47 <i>(7.8)</i>	2.78 <i>(13.4)</i>	2.13 <i>(9.3)</i>	1.59 <i>(7.4)</i>	1.60 <i>(7.7)</i>	1.74 <i>(8.3)</i>	1.65 <i>(7.4)</i>	1.43 <i>(6.4)</i>	1.37 <i>(7.8)</i>	1.77 <i>(8.2)</i>
Diesel Exhaust	3.35 <i>(16.8)</i>	2.47 <i>(13.1)</i>	2.93 <i>(14.1)</i>	3.77 <i>(16.5)</i>	3.61 <i>(16.9)</i>	3.11 <i>(15.0)</i>	3.43 <i>(16.4)</i>	3.70 <i>(16.6)</i>	2.72 <i>(12.1)</i>	2.22 <i>(12.6)</i>	3.13 <i>(14.6)</i>
Gasoline Exhaust	0.36 <i>(1.8)</i>	0.37 <i>(2.0)</i>	0.51 <i>(2.4)</i>	0.51 <i>(2.2)</i>	0.26 <i>(1.2)</i>	0.22 <i>(1.1)</i>	0.29 <i>(1.4)</i>	0.16 <i>(0.7)</i>	0.24 <i>(1.0)</i>	0.24 <i>(1.3)</i>	0.31 <i>(1.5)</i>
Sea Salt	1.57 <i>(7.9)</i>	1.84 <i>(9.7)</i>	1.92 <i>(9.2)</i>	1.80 <i>(7.8)</i>	1.76 <i>(8.2)</i>	1.64 <i>(7.9)</i>	1.47 <i>(7.0)</i>	1.33 <i>(6.0)</i>	1.38 <i>(6.1)</i>	1.77 <i>(10.1)</i>	1.65 <i>(7.7)</i>
Geological	0.83 <i>(4.2)</i>	0.83 <i>(4.4)</i>	0.87 <i>(4.2)</i>	1.45 <i>(6.3)</i>	1.23 <i>(5.7)</i>	1.45 <i>(7.0)</i>	1.32 <i>(6.3)</i>	2.03 <i>(9.1)</i>	0.81 <i>(3.6)</i>	0.80 <i>(4.6)</i>	1.16 <i>(5.4)</i>
Residual Oil Burning	1.30 <i>(6.5)</i>	0.82 <i>(4.4)</i>	0.51 <i>(2.5)</i>	0.43 <i>(1.9)</i>	0.39 <i>(1.8)</i>	0.33 <i>(1.6)</i>	0.29 <i>(1.4)</i>	0.28 <i>(1.3)</i>	0.27 <i>(1.2)</i>	0.52 <i>(2.9)</i>	0.51 <i>(2.4)</i>
Limestone									0.72 <i>(3.2)</i>		
Predicted Mass	19.98	18.89	20.83	22.89	21.42	20.73	20.93	22.33	22.50	17.65	21.46
Measured Mass	17.72	18.41	19.34	22.2	20.6	19.38	21.21	21.35	23.54	17.55	20.13

Italic, bold values in () are the percentages of predicted mass

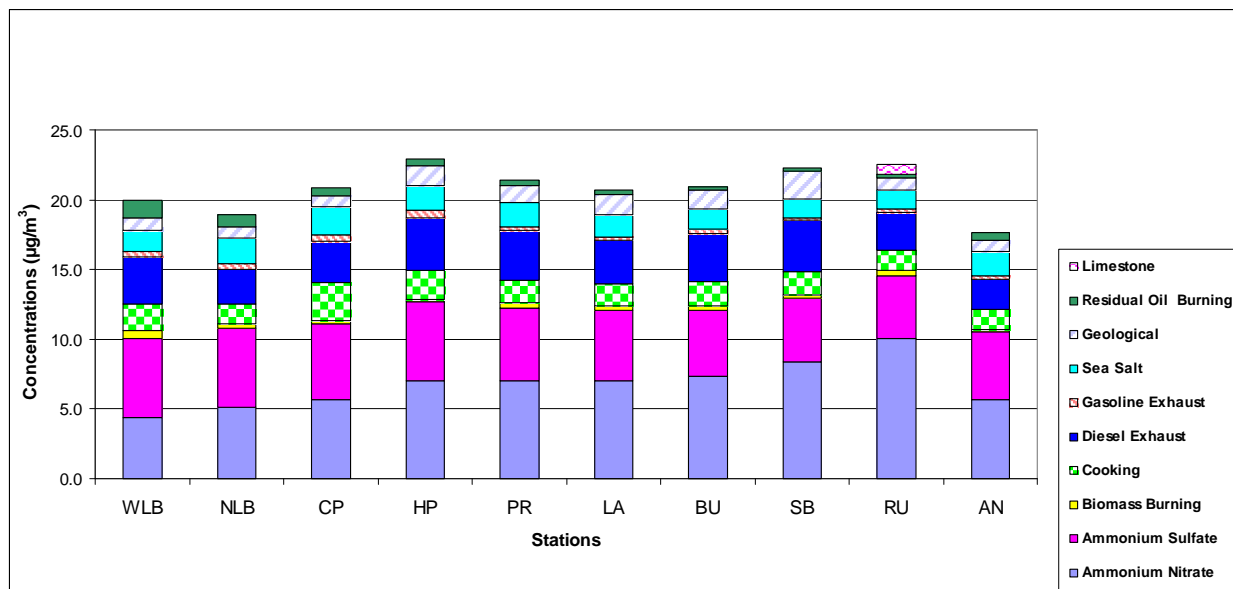


Figure VII-2. First-Year PM_{2.5} Source Contribution Estimates – Basin Gasoline Profile

The CMB estimated PM_{2.5} mass contributions range from 17.65 to 22.89 µg/m³ across the Basin. Major source contributors are ammonium nitrate (4.39 – 10.08 µg/m³, 22 – 44.8%), ammonium sulfate (4.49 – 5.68 µg/m³, 19.9 – 30%), biomass burning (0.15 – 0.57 µg/m³, 0.7 – 2.8%), cooking (1.37 – 2.78 µg/m³, 7.8 – 13.4%), diesel exhaust (2.22 – 3.77 µg/m³, 12.6 – 16.5%), gasoline exhaust (0.16 – 0.51 µg/m³, 0.7 – 2.4%), sea salt (1.33 – 1.92 µg/m³, 6.0 – 9.2%), geological (0.80 – 2.03 µg/m³, 4.6 – 9.1%), residual oil burning (0.27 – 1.30 µg/m³, 1.2 – 6.5%), and limestone (0.72 µg/m³, 3.2%) at the Rubidoux site.

The model performance statistics of the first year source apportionment (averaged R² values of 0.9 – 0.96; Chi² values of 2.02 – 3.12; and % difference in mass of 1 – 10%) are within the optimal performance ranges (R²: 0.8 – 1.0; Chi² ≤ 4.0; and % difference in mass ≤ 20%). Such optimal performance statistics indicate that the Basin gasoline profile is adequate for the CMB model.

However, high ratios of diesel to gasoline-exhaust contributions are observed across the Basin (from 5.75 in Compton to 23.13 in Inland Valley San Bernardino). The average diesel-gasoline ratio for all stations is 10.10, which is significantly higher than the 2007 AQMP diesel-gasoline emissions ratio of 1.90 and the ratio of 2.68 calculated from Fujita, et al.'s (2006) emission factors.

Source apportionment using the NFRAQS gasoline profile was therefore conducted, and the results are also presented in this analysis.

With the NFRAQS Gasoline Profile

A NFRAQS gasoline-vehicle profile used in the NFRAQS (Zielinska, et al. 1998) was applied to the CMB analysis.

The annual-average source contribution estimates of major PM_{2.5} source categories (in µg/m³) and their percentages of the total predicted mass are summarized in Table 2 and Figure 3.

Table VII-2
First-Year PM_{2.5} Source Contribution Estimates - NFRAQS Gasoline Profile

	WLB	NLB	CP	HP	PR	LA	BU	SB	RU	AN	10-Site Ave.
Ammonium Nitrate	4.40 <i>(21.0)</i>	5.14 <i>(26.2)</i>	5.69 <i>(26.0)</i>	7.00 <i>(29.3)</i>	7.03 <i>(32.0)</i>	7.04 <i>(33.2)</i>	7.33 <i>(34.0)</i>	8.43 <i>(37.2)</i>	10.08 <i>(44.0)</i>	5.70 <i>(31.3)</i>	6.78 <i>(30.7)</i>
Ammonium Sulfate	5.73 <i>(27.4)</i>	5.71 <i>(29.1)</i>	5.47 <i>(25.0)</i>	5.73 <i>(24.0)</i>	5.25 <i>(23.9)</i>	5.09 <i>(24.0)</i>	4.78 <i>(22.2)</i>	4.55 <i>(20.1)</i>	4.51 <i>(19.7)</i>	4.82 <i>(26.5)</i>	5.16 <i>(23.3)</i>
Biomass Burning	0.56 <i>(2.7)</i>	0.28 <i>(1.4)</i>	0.20 <i>(0.9)</i>	0.15 <i>(0.6)</i>	0.34 <i>(1.6)</i>	0.28 <i>(1.3)</i>	0.33 <i>(1.5)</i>	0.22 <i>(1.0)</i>	0.38 <i>(1.6)</i>	0.22 <i>(1.2)</i>	0.30 <i>(1.3)</i>
Cooking	1.93 <i>(9.2)</i>	1.49 <i>(7.6)</i>	2.88 <i>(13.2)</i>	2.17 <i>(9.1)</i>	1.59 <i>(7.2)</i>	1.61 <i>(7.6)</i>	1.76 <i>(8.2)</i>	1.72 <i>(7.6)</i>	1.44 <i>(6.3)</i>	1.39 <i>(7.6)</i>	1.80 <i>(8.1)</i>
Diesel Exhaust	3.25 <i>(15.5)</i>	2.20 <i>(11.2)</i>	2.67 <i>(12.2)</i>	3.34 <i>(14.0)</i>	3.30 <i>(15.0)</i>	2.85 <i>(13.4)</i>	3.18 <i>(14.8)</i>	3.51 <i>(15.5)</i>	2.54 <i>(11.1)</i>	2.10 <i>(11.5)</i>	2.89 <i>(13.1)</i>
Gasoline Exhaust	1.42 <i>(6.8)</i>	1.24 <i>(6.3)</i>	1.63 <i>(7.4)</i>	1.75 <i>(7.3)</i>	1.05 <i>(4.8)</i>	0.87 <i>(4.1)</i>	1.06 <i>(4.9)</i>	0.60 <i>(2.7)</i>	0.85 <i>(3.7)</i>	0.83 <i>(4.6)</i>	1.13 <i>(5.1)</i>
Sea Salt	1.58 <i>(7.5)</i>	1.84 <i>(9.4)</i>	1.90 <i>(8.7)</i>	1.79 <i>(7.5)</i>	1.76 <i>(8.0)</i>	1.64 <i>(7.7)</i>	1.47 <i>(6.8)</i>	1.33 <i>(5.9)</i>	1.38 <i>(6.0)</i>	1.76 <i>(9.7)</i>	1.64 <i>(7.4)</i>
Geological	0.79 <i>(3.8)</i>	0.87 <i>(4.5)</i>	0.95 <i>(4.3)</i>	1.49 <i>(6.3)</i>	1.26 <i>(5.8)</i>	1.49 <i>(7.0)</i>	1.35 <i>(6.3)</i>	2.00 <i>(8.8)</i>	0.78 <i>(3.4)</i>	0.85 <i>(4.7)</i>	1.19 <i>(5.4)</i>
Residual Oil Burning	1.28 <i>(6.1)</i>	0.83 <i>(4.2)</i>	0.52 <i>(2.4)</i>	0.43 <i>(1.8)</i>	0.39 <i>(1.8)</i>	0.33 <i>(1.5)</i>	0.29 <i>(1.4)</i>	0.28 <i>(1.2)</i>	0.27 <i>(1.2)</i>	0.53 <i>(2.9)</i>	0.51 <i>(2.3)</i>
Limestone									0.71 <i>(3.1)</i>		
Predicted Mass	20.94	19.59	21.91	23.85	21.98	21.20	21.55	22.64	22.93	18.20	21.40
Measured Mass	17.72	18.41	19.34	22.20	20.60	19.38	21.21	21.35	23.54	17.55	20.13

Italic, bold values in () are the percentages of predicted mass

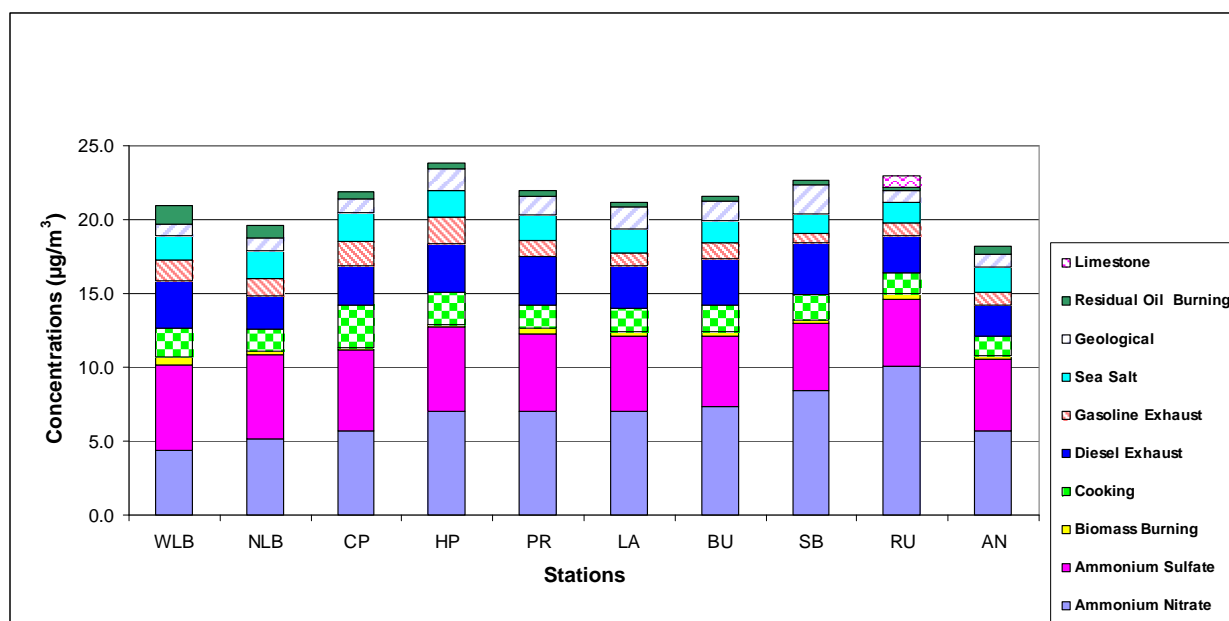


Figure VII-3. First-Year PM_{2.5} Source Contribution Estimates - NFRAQS Gasoline Profile

The CMB estimated PM_{2.5} mass contributions range from 18.20 to 23.85 µg/m³ across the Basin. Major source contributors are ammonium nitrate (4.40 – 10.08 µg/m³, 21 - 44%), ammonium sulfate (4.51 – 5.73 µg/m³, 19.7 – 27.4%), biomass burning (0.15 – 0.56 µg/m³, 0.6 – 2.7%), cooking (1.39 – 2.88 µg/m³, 7.6 – 13.2%), diesel exhaust (2.10 – 3.51 µg/m³, 11.6 – 15.5%), gasoline exhaust (0.6 – 1.75 µg/m³, 2.7 – 7.3%), sea salt (1.33 -1.9 µg/m³, 5.9 – 8.7%), geological (0.78 – 2.0 µg/m³, 3.4 – 8.8%), residual oil burning (0.27 – 1.28 µg/m³, 1.2 – 6.1%), and limestone (0.71 µg/m³, 3.1%) at the Rubidoux site.

The model performance statistics of the first year source apportionment (averaged R² values of 0.93 – 0.96; Chi² values of 2.02 – 2.94; and % difference in mass of 1 – 13%) are within the optimal performance ranges (R²: 0.8 – 1.0; Chi² ≤ 4.0; and % difference in mass ≤ 20%). Such optimal performance statistics indicate that the NFRAQS gasoline profile is also adequate for the CMB model.

The ratios of diesel to gasoline-exhaust contributions across the Basin vary from 1.64 in Compton to 5.80 in Inland Valley San Bernardino. The average diesel to gasoline ratio for all stations is 2.56, which is within the range of the 2007 AQMP diesel-gasoline emissions ratio of 1.90 and the ratio of 2.68 calculated from Fujita, et al.’s (2006) emission factors.

Basin and NFRAQS Gasoline Profiles Comparison

Figure 4 compares the first-year contributions of major sources averaged among ten sites, using both Basin and NFRAQS gasoline profiles.

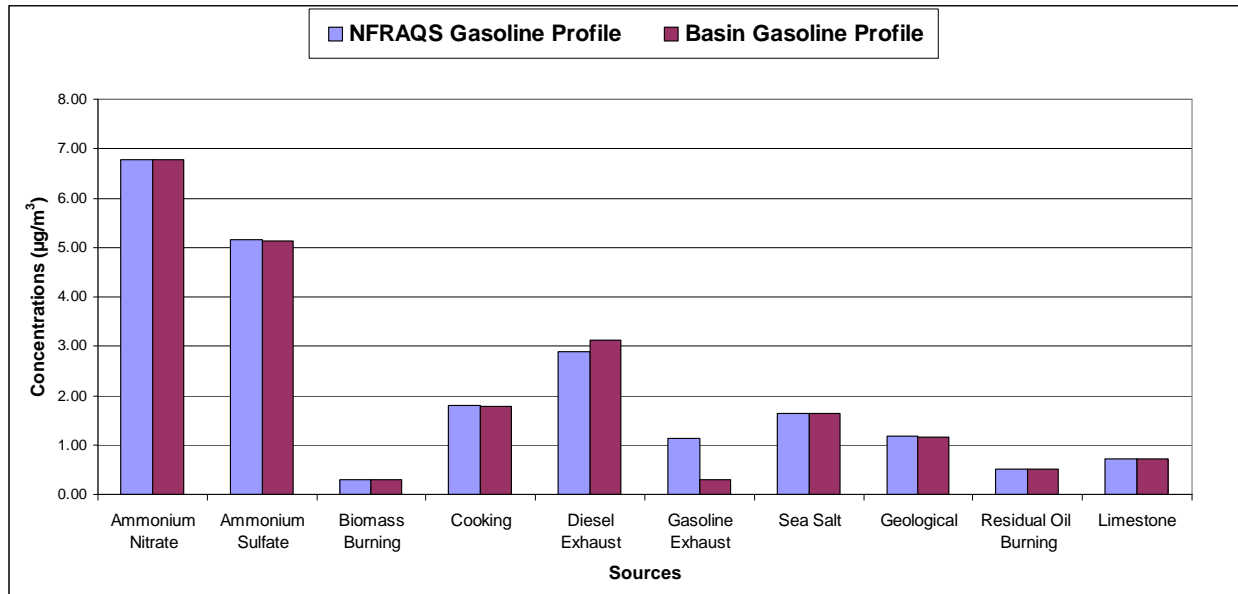


Figure VII-4. First-Year – 10-Site Average Sources Comparison

Applying the Basin gasoline profile affects other sources only slightly, but greatly impacts gasoline exhaust contributions. The 10-site average contribution from diesel exhaust went from 3.13 µg/m³ with the Basin gasoline mobile to 2.89 µg/m³ with the NFRAQS gasoline

profile, a difference of 7.7%. Using the Basin gasoline profile also results in similar spatial contribution pattern as using the NFRAQS profile.

Spatial Analysis

The following discussion on spatial and seasonal differences is apportioned mass below focuses on the apportionment using the NFRAQS gasoline profile. Ammonium nitrate displays a strong spatial variation, with high contributions inland and low contributions in coastal areas. Ammonium nitrate varies between $4.4 \mu\text{g}/\text{m}^3$ (21%) in West Long Beach and $10.08 \mu\text{g}/\text{m}^3$ (44%) in Rubidoux. Nitric acid concentration increases to the highest level at Diamond Bar that is located upwind of a dense array of dairy ammonia source (Kim, et. al. 2000). Most of the nitric acid is then neutralized by ammonia while transported to downwind locations that results in high ammonium nitrate contribution in Rubidoux.

Ammonium sulfate also shows a strong spatial variation, but in contrast to ammonium nitrate, with high contributions in coastal areas and low contributions inland. Ammonium sulfate varies between $5.73 \mu\text{g}/\text{m}^3$ (27.4%) in West Long Beach and $4.51 \mu\text{g}/\text{m}^3$ (19.7%) in Rubidoux. Greater RH ($\geq 75\%$) at the coastal sites and the importance of the aqueous-phase sulfate chemistry at high RH may explain the higher sulfate contributions at coastal sites.

Biomass burning does not show a clear spatial variation. The highest contribution is observed at West Long Beach ($0.56 \mu\text{g}/\text{m}^3$, 2.7%) and the lowest contribution is observed at Huntington Park ($0.15 \mu\text{g}/\text{m}^3$, 0.6 %).

Cooking does not display a clear spatial variation. The highest contribution is observed at Compton ($2.88 \mu\text{g}/\text{m}^3$, 13.2%) and the lowest contribution is observed at Anaheim ($1.39 \mu\text{g}/\text{m}^3$, 7.6%). The highest cooking concentration at Compton may be biased since the monitoring station is located above the county fire station where cooking activities might occur during the sampling period.

Diesel exhaust displays high contributions in West Long Beach ($3.25 \mu\text{g}/\text{m}^3$, 15.5%), which is within close proximity to the ports and cargo distribution centers, and at industrial areas, such as Huntington Park ($3.34 \mu\text{g}/\text{m}^3$, 14%), Burbank ($3.18 \mu\text{g}/\text{m}^3$, 14.8%), Inland Valley San Bernardino ($3.51 \mu\text{g}/\text{m}^3$, 15.5%), and Pico Rivera ($3.3 \mu\text{g}/\text{m}^3$, 15%) where heavy diesel-truck traffic occurs. The lowest diesel contribution is observed at Anaheim ($2.10 \mu\text{g}/\text{m}^3$, 11.5%).

The highest gasoline exhaust contribution is observed at Huntington Park ($1.75 \mu\text{g}/\text{m}^3$, 7.3%) and the lowest contribution is observed at Inland Valley San Bernardino ($0.60 \mu\text{g}/\text{m}^3$, 2.7%). Gasoline exhaust displays higher contributions at the ports and in more urbanized areas where dense population and heavy gasoline-vehicle traffic are located; however, gasoline estimate for Los Angeles ($0.87 \mu\text{g}/\text{m}^3$, 4.1%) is relatively lower than other urbanized areas.

Sea salt shows a spatial variation with high contributions in coastal areas and low contributions inland. The highest contribution is observed at Compton ($1.90 \mu\text{g}/\text{m}^3$, 8.7%) and the lowest contribution is observed in Inland Valley San Bernardino ($1.33 \mu\text{g}/\text{m}^3$, 5.9%).

Geological shows a strong spatial variation with low contributions in coastal areas and high contributions inland. The lowest contribution is observed at West Long Beach ($0.79 \mu\text{g}/\text{m}^3$, 3.8%) and the highest contribution ($2.0 \mu\text{g}/\text{m}^3$, 8.8%) is observed at Inland Valley San Bernardino where high winds cause more re-suspended soil dust.

Limestone is the only other source contributing to $\text{PM}_{2.5}$ mass at Rubidoux. The geological source alone was not sufficient to explain the high measured ambient calcium concentrations in Rubidoux. Addition of limestone source in the CMB analysis accounted for the excess calcium. These findings are consistent with earlier studies (Chow, et. al., 1992; Kim, et. al., 1992).

Residual oil burning displays a strong spatial variation. The highest residual oil burning contribution ($1.28 \mu\text{g}/\text{m}^3$, 6.1%) is observed in West Long Beach where shipping activities occur. The contributions remain higher in the surrounding coastal areas in relation to the inland. The lowest contribution is observed at Rubidoux ($0.27 \mu\text{g}/\text{m}^3$, 1.2%).

Seasonal Analysis

Ammonium nitrate displays a seasonal variation. The highest contribution is observed in the fall (September through November) as shown in Figure 5. Cool temperatures and stagnant conditions favor the formation of ammonium nitrate (Appel, et al., 1980, Stelson and Seinfeld, 1982, Russel, et al., 1983). The average ammonium nitrate among the 10 monitoring sites varies between $5.51 \mu\text{g}/\text{m}^3$ in the winter (December through February) and $8.23 \mu\text{g}/\text{m}^3$ in the fall.

As depicted in Figure 5, ammonium sulfate displays a clear seasonal variation. Unlike ammonium nitrate, the highest ammonium sulfate contribution is observed in the summer (June through August) and the lowest contribution in the winter. The average ammonium sulfate among 10 sites varies between $1.99 \mu\text{g}/\text{m}^3$ and $8.70 \mu\text{g}/\text{m}^3$.

Biomass burning shows a strong seasonal variation as shown in Figure 5. The highest contributions are observed in the fall and winter when more heating activities and lower ambient air mixing height occur. The average biomass burning among 10 sites varies between $0.11 \mu\text{g}/\text{m}^3$ in the summer and $0.38 \mu\text{g}/\text{m}^3$ in the fall and winter.

As illustrated in Figure 6, although cooking does not show a clear seasonal variation, the highest cooking contribution is observed in the winter when ambient air mixing height is low. The average cooking among 10 sites varies between $1.10 \mu\text{g}/\text{m}^3$ in the summer and $2.23 \mu\text{g}/\text{m}^3$ in the winter.

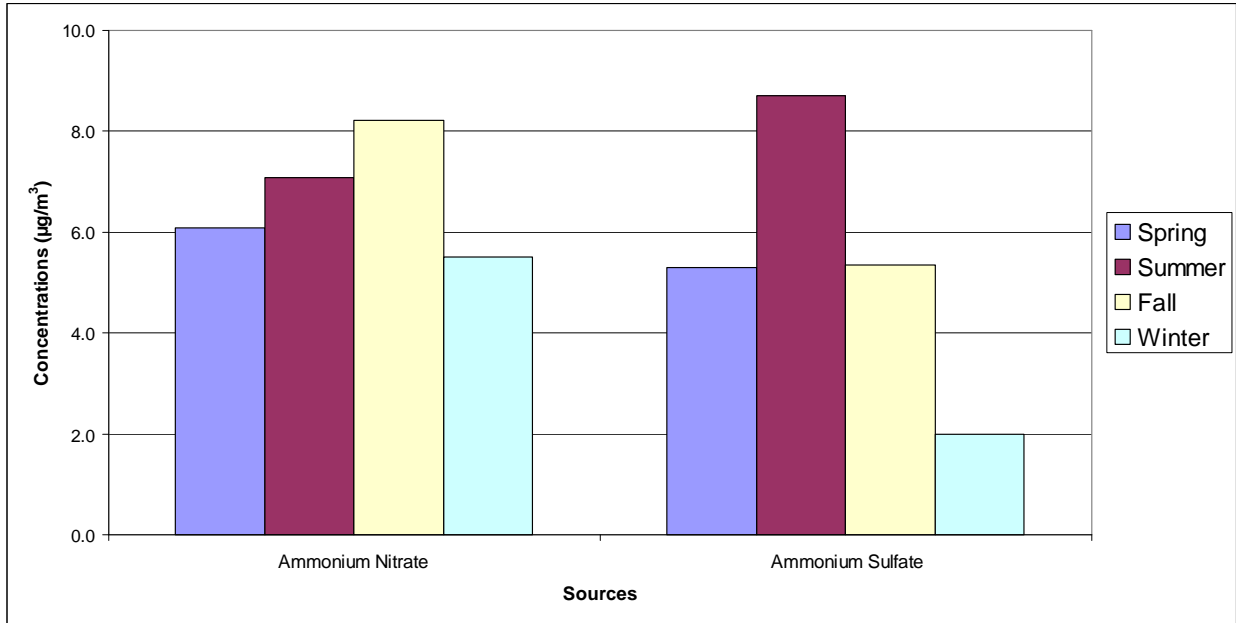


Figure VII-5. First Year 10-Site Average Seasonal Contributions – Ammonium Nitrate and Sulfate

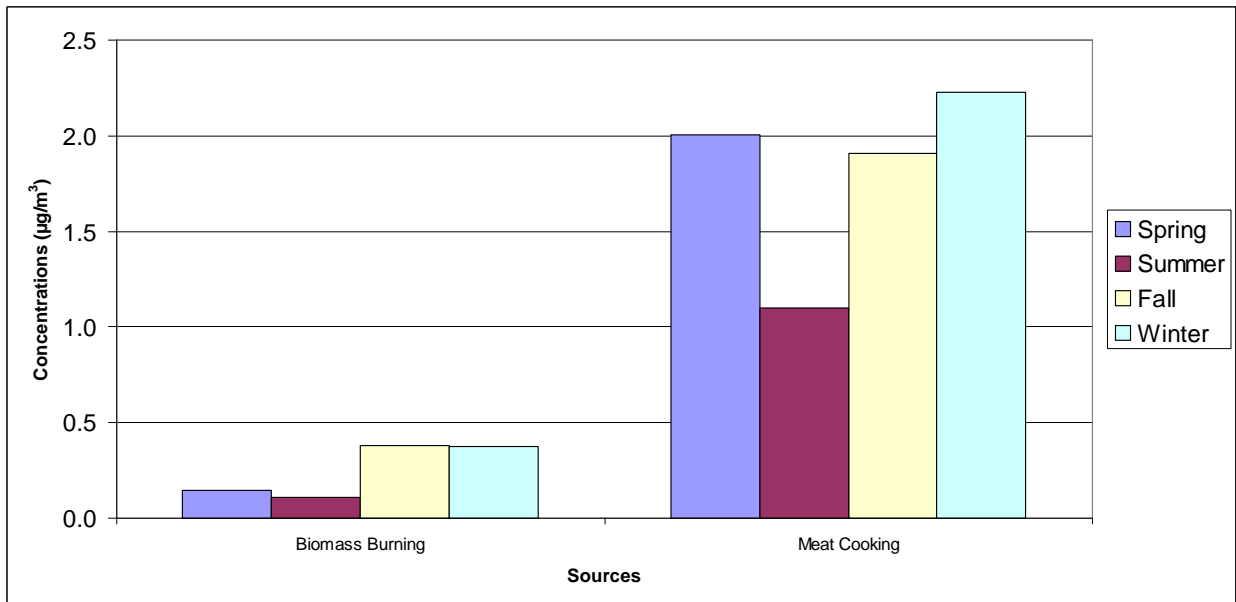


Figure VII-6. First Year 10-Site Average Seasonal Contributions – Biomass Burning and Cooking

Diesel exhaust displays a strong seasonal variation as shown in Figure 7. The highest contribution is observed in the winter when ambient air mixing height is low. The average diesel-vehicle exhaust among 10 sites varies between $1.86 \mu\text{g}/\text{m}^3$ in the spring (April and May) and $4.13 \mu\text{g}/\text{m}^3$ in the winter.

As with diesel exhaust, the highest gasoline contribution ($1.62 \mu\text{g}/\text{m}^3$) is also found in the winter when ambient air mixing height is low. As shown in Figure 7, the lower contributions ($0.8 \mu\text{g}/\text{m}^3$ and $0.91 \mu\text{g}/\text{m}^3$) are observed in the summer and fall, respectively.

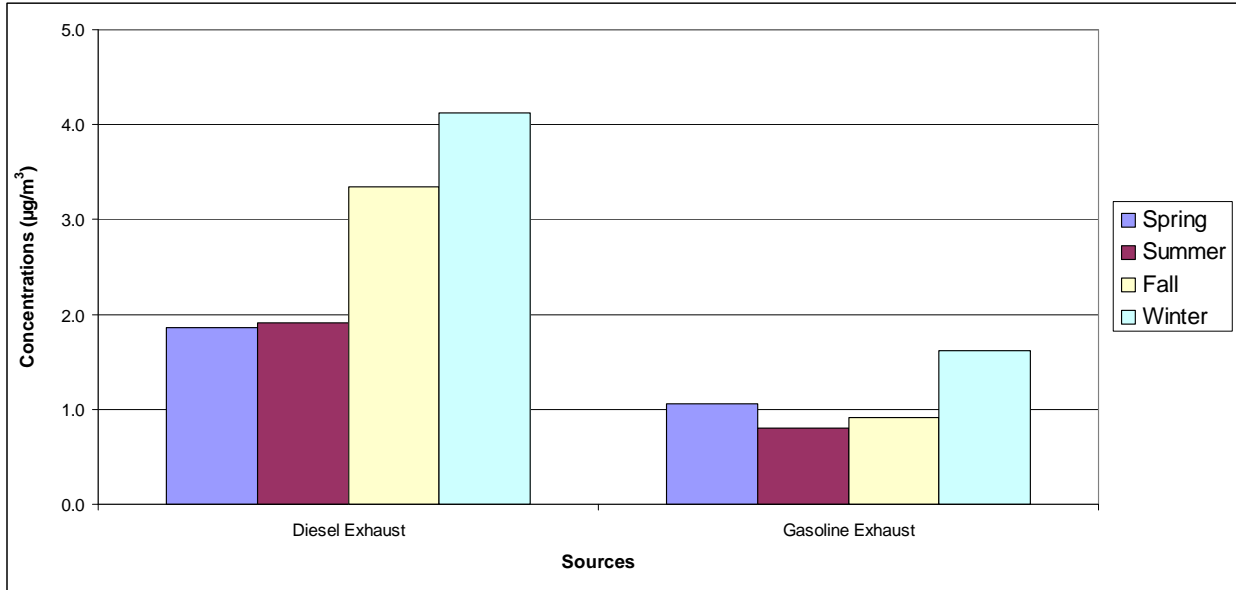
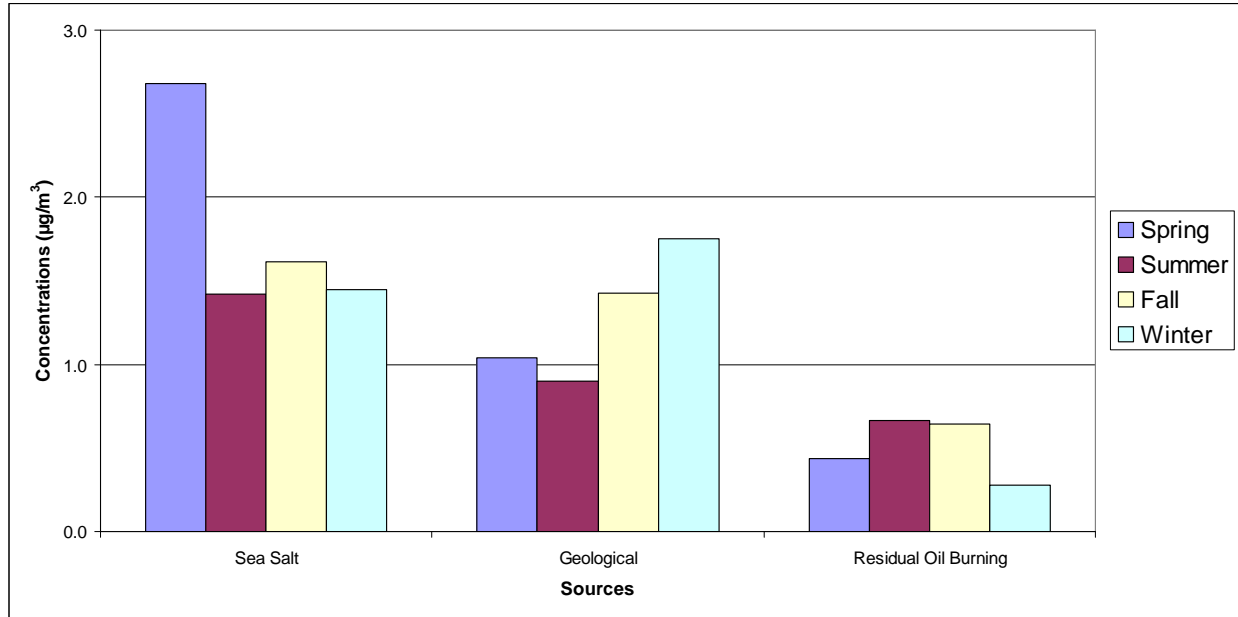


Figure VII-7. 10-Site Average First-Year Seasonal Contributions – Diesel and Gasoline Exhaust

As depicted in Figure 8, the highest sea salt contribution ($2.68 \mu\text{g}/\text{m}^3$) is observed in the spring when land and sea temperature differential is higher, resulting in stronger offshore winds that create greater sea spray. The lowest contribution ($1.42 \mu\text{g}/\text{m}^3$) is observed in the summer.



**Figure VII-8. 10-Site Average First-year Seasonal Contributions
Sea Salt, Geological, and Residual Oil Burning**

Geological shows a strong seasonal variation where the highest contribution ($1.75 \mu\text{g}/\text{m}^3$) is observed in the winter, the strong winds season. The lowest contribution ($0.90 \mu\text{g}/\text{m}^3$) is in the summer as shown in Figure 8.

Residual oil burning also displays a strong seasonal variation as shown in Figure 8. The highest contributions are observed in the summer and fall ($0.67 \mu\text{g}/\text{m}^3$ and $0.65 \mu\text{g}/\text{m}^3$, respectively), and the lowest contribution ($0.28 \mu\text{g}/\text{m}^3$) in the winter.

April 2005 to April 2006 (Second-Year) $\text{PM}_{2.5}$ Source Apportionment

The following $\text{PM}_{2.5}$ source apportionment was conducted independently for the second year, using the same source profiles and fitting species.

With the Basin Gasoline Profile

The annual-averaged source contribution estimates of major $\text{PM}_{2.5}$ source categories (in $\mu\text{g}/\text{m}^3$) and their percentage of the total predicted mass are summarized in Table 3 and Figure 9.

Table VII-3
Second-Year PM_{2.5} Source Contribution Estimates - Basin Gasoline Profile

	WLB	NLB	CP	LA	BU	SB	RU	AN	8-Site Average
Ammonium Nitrate	4.56 <i>(24.0)</i>	4.92 <i>(28.6)</i>	5.50 <i>(29.6)</i>	6.55 <i>(34.0)</i>	6.69 <i>(33.3)</i>	8.55 <i>(37.9)</i>	10.23 <i>(45.0)</i>	5.39 <i>(31.2)</i>	6.55 <i>(32.2)</i>
Ammonium Sulfate	4.94 <i>(25.9)</i>	4.90 <i>(28.5)</i>	4.31 <i>(23.3)</i>	4.04 <i>(21.0)</i>	3.91 <i>(19.5)</i>	3.63 <i>(16.1)</i>	3.68 <i>(16.2)</i>	3.90 <i>(22.6)</i>	4.16 <i>(20.5)</i>
Biomass Burning	0.32 <i>(1.7)</i>	0.38 <i>(2.2)</i>	0.42 <i>(2.2)</i>	0.42 <i>(2.2)</i>	0.46 <i>(2.3)</i>	0.39 <i>(1.7)</i>	0.43 <i>(1.9)</i>	0.39 <i>(2.3)</i>	0.40 <i>(2.0)</i>
Cooking	1.21 <i>(6.4)</i>	0.98 <i>(5.7)</i>	1.63 <i>(8.8)</i>	1.24 <i>(6.4)</i>	1.47 <i>(7.3)</i>	1.45 <i>(6.4)</i>	1.34 <i>(5.9)</i>	1.43 <i>(8.3)</i>	1.34 <i>(6.6)</i>
Diesel-Exhaust	4.25 <i>(22.4)</i>	2.90 <i>(16.9)</i>	3.34 <i>(18.0)</i>	4.46 <i>(23.2)</i>	4.09 <i>(20.4)</i>	4.77 <i>(21.1)</i>	4.02 <i>(17.7)</i>	2.89 <i>(16.7)</i>	3.84 <i>(18.9)</i>
Gasoline-Exhaust	0.30 <i>(1.6)</i>	0.25 <i>(1.4)</i>	0.45 <i>(2.4)</i>	0.24 <i>(1.3)</i>	0.31 <i>(1.5)</i>	0.16 <i>(0.7)</i>	0.21 <i>(0.9)</i>	0.19 <i>(1.1)</i>	0.26 <i>(1.3)</i>
Sea Salt	1.50 <i>(7.9)</i>	1.46 <i>(8.5)</i>	1.43 <i>(7.7)</i>	1.11 <i>(5.8)</i>	1.01 <i>(5.0)</i>	1.07 <i>(4.7)</i>	1.09 <i>(4.8)</i>	1.30 <i>(7.5)</i>	1.25 <i>(6.1)</i>
Geological	0.62 <i>(3.2)</i>	0.68 <i>(3.9)</i>	0.97 <i>(5.2)</i>	0.82 <i>(4.3)</i>	1.86 <i>(9.2)</i>	2.21 <i>(9.8)</i>	0.62 <i>(2.7)</i>	1.28 <i>(7.4)</i>	1.13 <i>(5.6)</i>
Residual Oil Burning	1.31 <i>(6.9)</i>	0.72 <i>(4.2)</i>	0.51 <i>(2.7)</i>	0.38 <i>(1.9)</i>	0.30 <i>(1.5)</i>	0.35 <i>(1.6)</i>	0.27 <i>(1.2)</i>	0.48 <i>(2.8)</i>	0.54 <i>(2.6)</i>
Limestone							0.87 <i>(3.8)</i>		
Predicted Mass	18.96	17.18	18.55	19.27	20.08	22.58	22.76	17.25	19.47
Measured Mass	18.10	16.74	17.66	17.40	19.97	20.98	21.80	16.81	18.68

Italic, bold values in () are the percentages of predicted mass

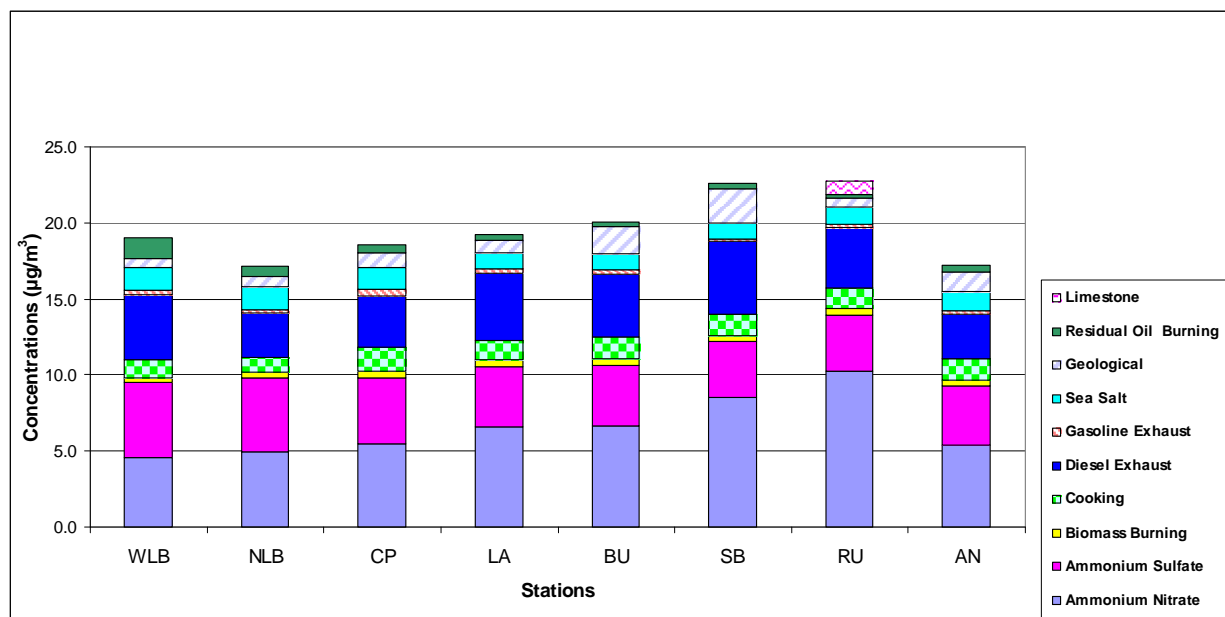


Figure VII-9. Second-Year PM_{2.5} Source Contribution Estimates - Basin Gasoline Profile

Major source contributors are ammonium nitrate (4.56 – 10.23 µg/m³, 24.0 – 45.0%), ammonium sulfate (3.63 – 4.94 µg/m³, 16.1 – 28.5%), biomass burning (0.32 – 0.46 µg/m³, 1.7 –

2.3%), cooking (0.98 – 1.63 $\mu\text{g}/\text{m}^3$, 5.7 – 8.8%), diesel-exhaust (2.89 – 4.77 $\mu\text{g}/\text{m}^3$, 16.7 – 21.1%), gasoline-vehicle exhaust (0.16 – 0.45 $\mu\text{g}/\text{m}^3$, 0.7 – 2.4%), sea salt (1.01 – 1.5 $\mu\text{g}/\text{m}^3$, 5.0 – 7.9%), geological (0.62 – 2.21 $\mu\text{g}/\text{m}^3$, 2.7 – 9.8%), residual oil burning (0.27 – 1.31 $\mu\text{g}/\text{m}^3$, 1.2 – 6.9%), and limestone (0.87 $\mu\text{g}/\text{m}^3$, 3.8%) at the Rubidoux site.

With the NFRAQS Gasoline Profile

The annual-averaged source contribution estimates of major PM_{2.5} source categories (in $\mu\text{g}/\text{m}^3$) and their percentage of the total predicted mass are summarized in Table 4 and Figure 10.

The CMB estimated PM_{2.5} mass contributions range from 17.74 to 23.16 $\mu\text{g}/\text{m}^3$ across the Basin. Major source contributors are ammonium nitrate (4.56 – 10.24 $\mu\text{g}/\text{m}^3$, 22.9 – 44.2%), ammonium sulfate (3.65 – 4.94 $\mu\text{g}/\text{m}^3$, 15.8 – 29.4%), biomass burning (0.32 – 0.46 $\mu\text{g}/\text{m}^3$, 1.6 – 2.2%), cooking operations (0.98 – 1.66 $\mu\text{g}/\text{m}^3$, 5.5 – 8.5%), diesel-vehicle exhaust (2.6 – 4.63 $\mu\text{g}/\text{m}^3$, 14.6 – 20.1%), gasoline-vehicle exhaust (0.73 – 1.75 $\mu\text{g}/\text{m}^3$, 3.2 – 8.8%), sea salt (1.01 – 1.53 $\mu\text{g}/\text{m}^3$, 4.8 – 7.7%), geological (0.64 – 2.23 $\mu\text{g}/\text{m}^3$, 3.2 – 9.7%), residual oil burning (0.26 – 1.29 $\mu\text{g}/\text{m}^3$, 1.1 – 6.5%), and limestone (0.85 $\mu\text{g}/\text{m}^3$, 3.7%).

Table VII-4
Second-Year PM_{2.5} Source Contribution Estimates – NFRAQS Gasoline Profile

	WLB	NLB	CP	LA	BU	SB	RU	AN	8-Sites Average
Ammonium Nitrate	4.56 (22.9)	4.92 (27.5)	5.50 (28.2)	6.55 (33.3)	6.69 (32.0)	8.55 (37.1)	10.24 (44.2)	5.39 (30.4)	6.55 (31.2)
Ammonium Sulfate	4.94 (29.4)	4.92 (27.5)	4.35 (22.3)	4.06 (20.6)	3.94 (18.8)	3.65 (15.8)	3.72 (16.0)	3.92 (22.1)	4.19 (20.0)
Biomass Burning	0.32 (1.6)	0.38 (2.1)	0.42 (2.1)	0.42 (2.1)	0.46 (2.2)	0.39 (1.7)	0.43 (1.9)	0.39 (2.2)	0.40 (1.9)
Cooking	1.21 (6.1)	0.98 (5.5)	1.66 (8.5)	1.26 (6.4)	1.49 (7.1)	1.47 (6.4)	1.33 (5.8)	1.44 (8.1)	1.36 (6.5)
Diesel-Exhaust	3.64 (18.3)	2.60 (14.6)	3.09 (15.9)	4.19 (21.3)	3.86 (18.5)	4.63 (20.1)	3.49 (15.1)	2.65 (15.0)	3.52 (16.8)
Gasoline-Exhaust	1.75 (8.8)	1.19 (6.7)	1.52 (7.8)	0.91 (4.6)	1.27 (6.1)	0.73 (3.2)	1.07 (4.6)	0.86 (4.8)	1.16 (5.5)
Sea Salt	1.53 (7.7)	1.45 (8.1)	1.43 (7.3)	1.14 (5.8)	1.01 (4.8)	1.07 (4.6)	1.10 (4.7)	1.30 (7.3)	1.25 (6.0)
Geological	0.64 (3.2)	0.71 (4.0)	1.01 (5.2)	0.80 (4.1)	1.89 (9.0)	2.23 (9.7)	0.68 (2.9)	1.30 (7.3)	1.16 (5.5)
Residual Oil Burning	1.29 (6.5)	0.72 (4.0)	0.51 (2.6)	0.38 (1.9)	0.30 (1.4)	0.35 (1.5)	0.26 (1.1)	0.48 (2.7)	0.54 (2.6)
Limestone							0.85 (3.7)		
Predicted Mass	19.89	17.88	19.49	19.70	21.16	23.07	23.16	17.74	20.13
Measured Mass	18.10	16.74	17.66	17.40	19.97	20.98	21.8	16.8	18.68

Italic, bold values in () are the percentages of predicted mass

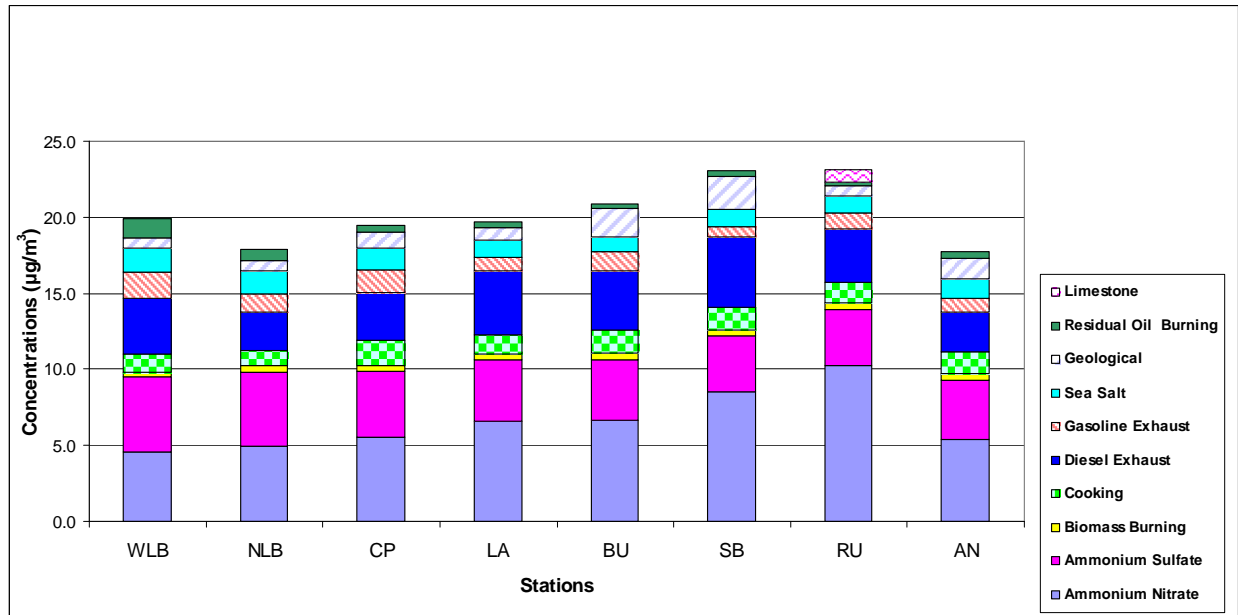


Figure VII-10. Second-Year PM_{2.5} Source Contribution Estimates – NFRAQS Gasoline Profile

Basin and NFRAQS Gasoline Profiles Comparison

Figure 11 compares the second-year contributions of major sources averaged among eight sites, using both Basin and NFRAQS gasoline profiles.

Similar to the first-year source apportionment, applying the Basin gasoline profile to the second-year ambient data affects other sources only slightly, but greatly impacts gasoline exhaust contributions. Using the Basin gasoline profile also results in similar spatial contribution pattern as using the NFRAQS profile.

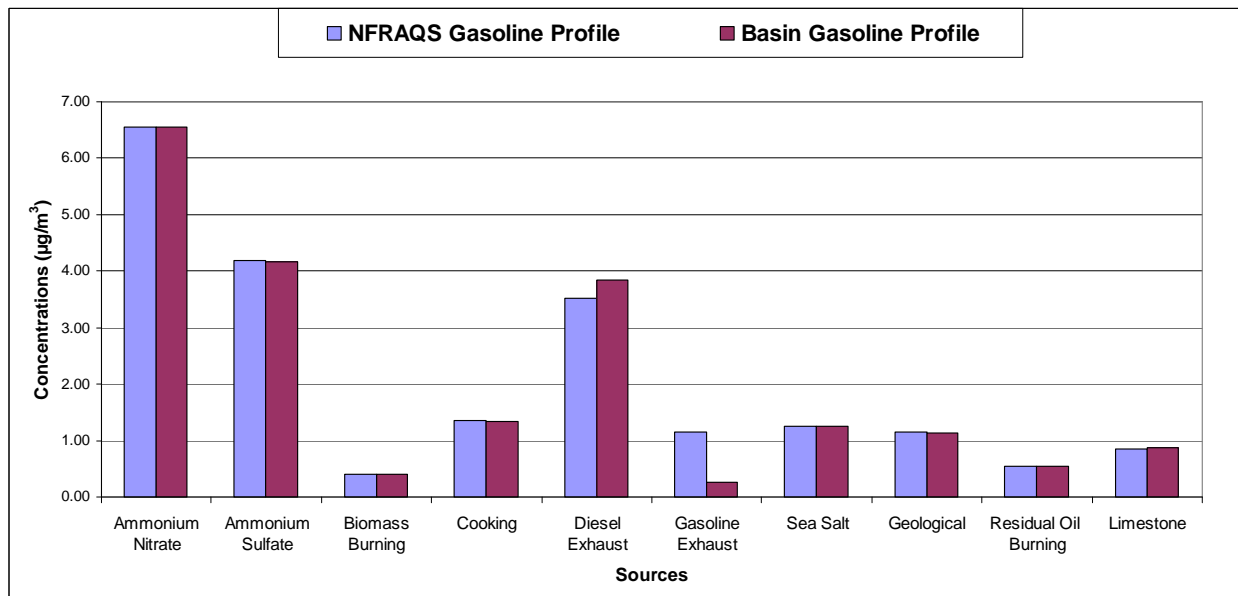


Figure 11. Second-Year 8-Site Average Sources Comparison

First and Second-Year Source Apportionment Comparisons

With the Basin Gasoline Profile

Figure 12 compares the major source contributions at all stations during the two years.

PM_{2.5} mass slightly decreased in the second year. However, elemental carbon (EC) concentration increased in the second year, resulting in increased diesel-vehicle contributions. Higher EC concentrations coincide with increased diesel trucking activities during the second year. According to the ARB’s EMFAC data (2007), the vehicle-miles-traveled (VMT) for diesel vehicles in 2004 was 16,398,000, while in 2005 the VMT increased to 18,608,000 (a 13% increase).

Second-year source contributions are very similar to the first-year source contributions except diesel-vehicle contributions. As a result, the ratios of diesel to gasoline-vehicle contributions across the Basin vary from 7.4 in Compton to 30.7 in Inland Valley San Bernardino. The average diesel to gasoline ratio for all stations is 14.6, which is higher than the first-year ratio of 10.0, and significantly higher than the 2007 AQMP diesel-gasoline emissions ratio of 1.90 and the ratio of 2.68 calculated from Fujita, et al.’s (2006) emission factors.

The second-year spatial contribution pattern is similar to that of the first year.

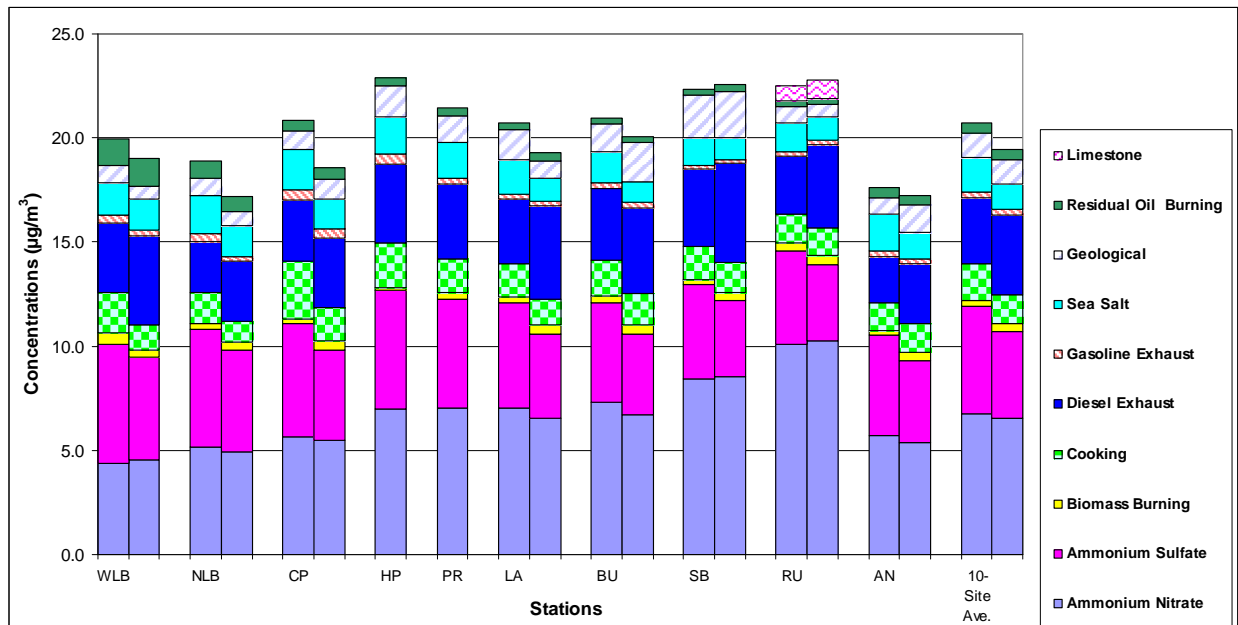


Figure VII-12. First & Second-Year PM_{2.5} Source Contribution Comparison Basin Gasoline Profile

With the NFRAQS Gasoline Profile

Figure 13 compares the major source contributions at all stations during the two years.

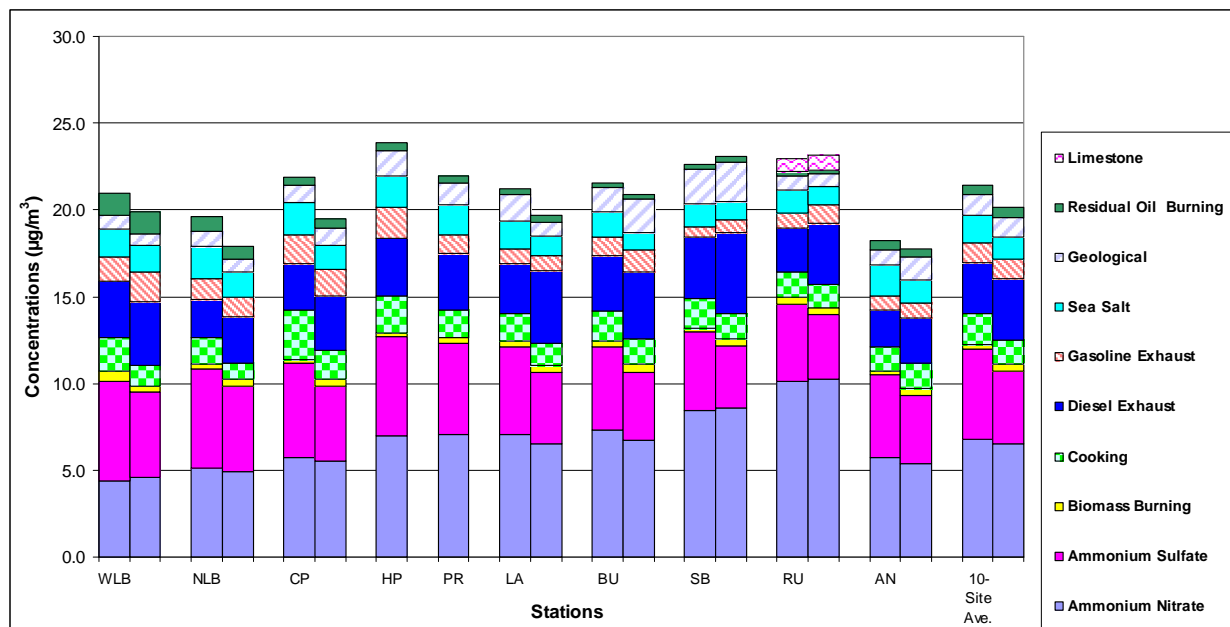


Figure VII-13. First & Second-Year PM_{2.5} Source Contribution Comparison NFRAQS Gasoline Profile

PM_{2.5} mass also slightly decreased in the second year. Second-year source contributions are very similar to the first-year source contributions, except diesel-vehicle contributions. As a result, the ratios of diesel to gasoline-vehicle contributions across the Basin vary from 2.03 in Compton to 6.33 in Inland Valley San Bernardino, which is higher than the first-year ratio due to the higher second-year diesel contribution. The average diesel-gasoline ratio for all stations is 3.03, which is slightly higher than the 2007 AQMP diesel-gasoline emissions ratio of 1.90 and the ratio of 2.68 calculated from Fujita, et al.'s (2006) emission factors.

The second-year spatial contribution pattern is also similar to that of the first year.

VII-3 SENSITIVITY TESTS

Sensitivity tests have been conducted not only for gasoline, but also for diesel exhaust, biomass burning, and cooking, using various profiles. In the sensitivity tests, major chemical species in various profiles were modified and/or different profile combinations were used to evaluate model performance.

In the beginning, various NFRAQS diesel profiles were applied to determine model performance. However, the poor performance statistics (e.g., R^2 , χ^2 , etc.) obtained indicated that these diesel profiles were not appropriate for the model. Therefore, their applications were not continued, and the Basin diesel profile was selected.

Cooking sensitivity tests were also conducted using various profiles developed by Desert Research Institute (DRI) for use in the Fresno Supersite. However, due to the poor model statistics obtained, their sensitivity applications were not continued.

A biomass burning profile that was developed by DRI for the Fresno Supersite was applied to the CMB analysis, along with the NFRAQS gasoline and other profiles used throughout this study, for comparison purposes. In general, contributions of all source categories are affected slightly by this profile, except for biomass burning.

Figures 14, 15, and 16, respectively show that, using the DRI profile, biomass burning contributions for Los Angeles, West Long Beach, and Rubidoux are approximately two times greater than the current contributions using the Basin profile (Schauer, 1998). However, the CMB model performance statistics, that is, the chi-square values generated from using the DRI profile are roughly 1.5 times greater than that from using the Basin profile. The biomass burning contribution of $0.72 \mu\text{g}/\text{m}^3$ in Rubidoux using the DRI profile (vs. $0.38 \mu\text{g}/\text{m}^3$ using the Basin profile) is similar to the $0.79 \mu\text{g}/\text{m}^3$ estimated by the PMF for data collected between 2001 and 2004 at U.S. EPA Speciation Trends Network monitoring site in Rubidoux (Kim and Hopke, 2007). However, the 4-month averaged biomass burning contribution of $0.84 \mu\text{g}/\text{m}^3$ from November to February in Rubidoux using the DRI profile (vs. $0.36 \mu\text{g}/\text{m}^3$ using the Basin profile) is lower than ARB's $1.8 - 2.2 \mu\text{g}/\text{m}^3$ estimated by their 1995 CMB and 2005 PMF models, respectively (ARB, 2007).

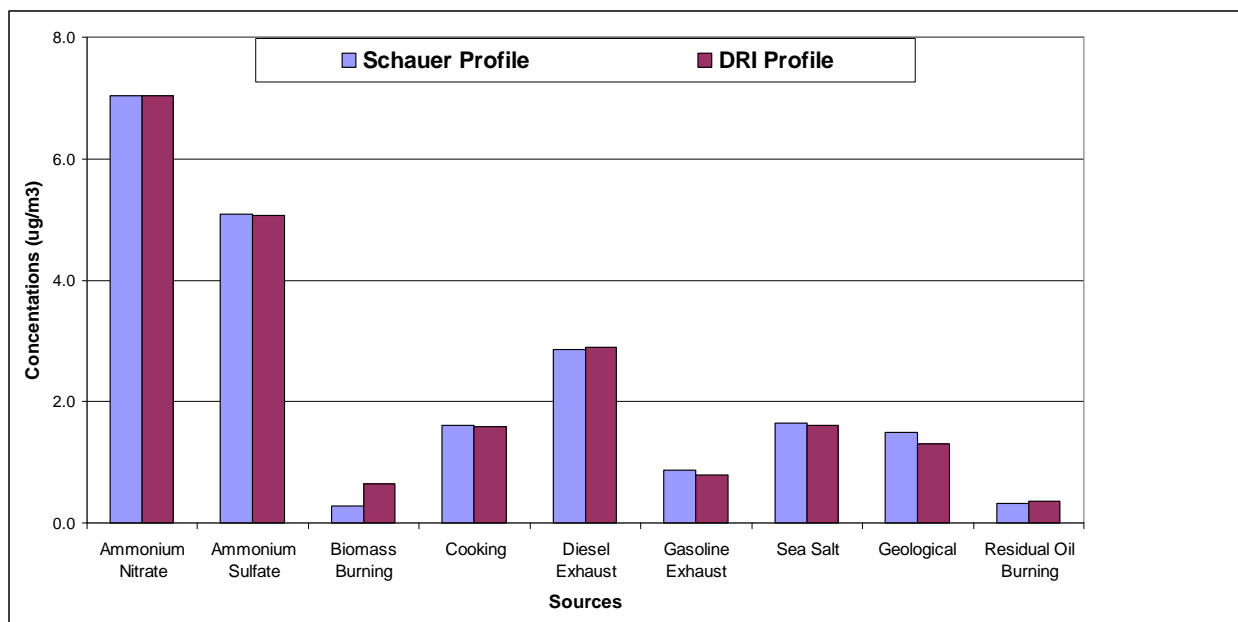


Figure VII-14. Los Angeles PM_{2.5} Source Contributions – Using Different Biomass Burning Profiles

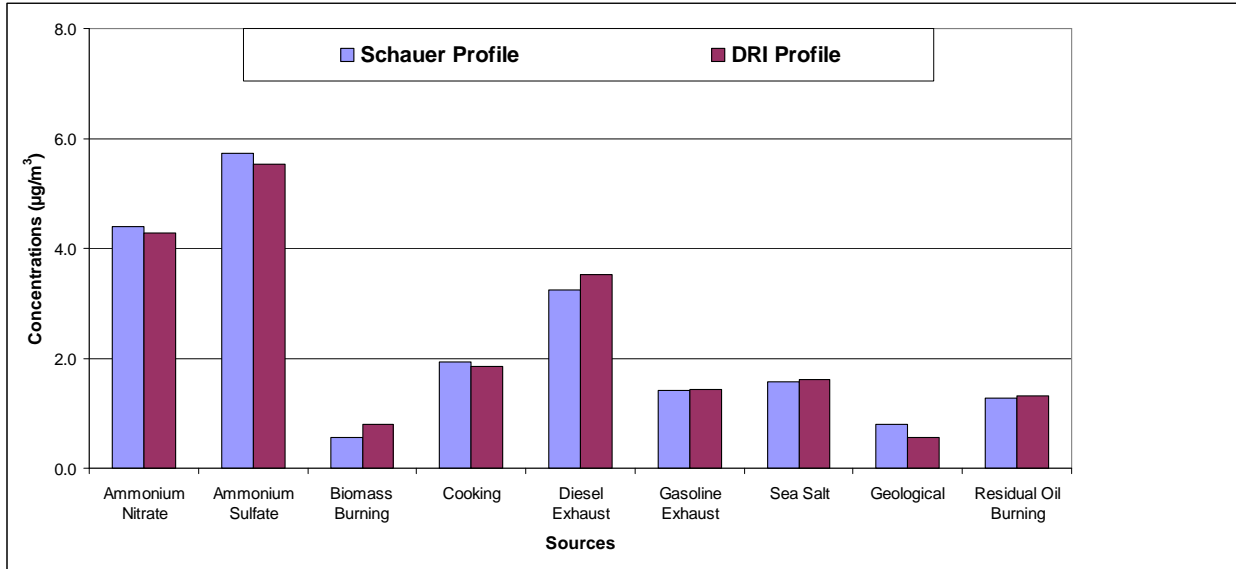


Figure VII-15. West Long Beach PM_{2.5} Source Contributions – Using Different Biomass Burning Profiles

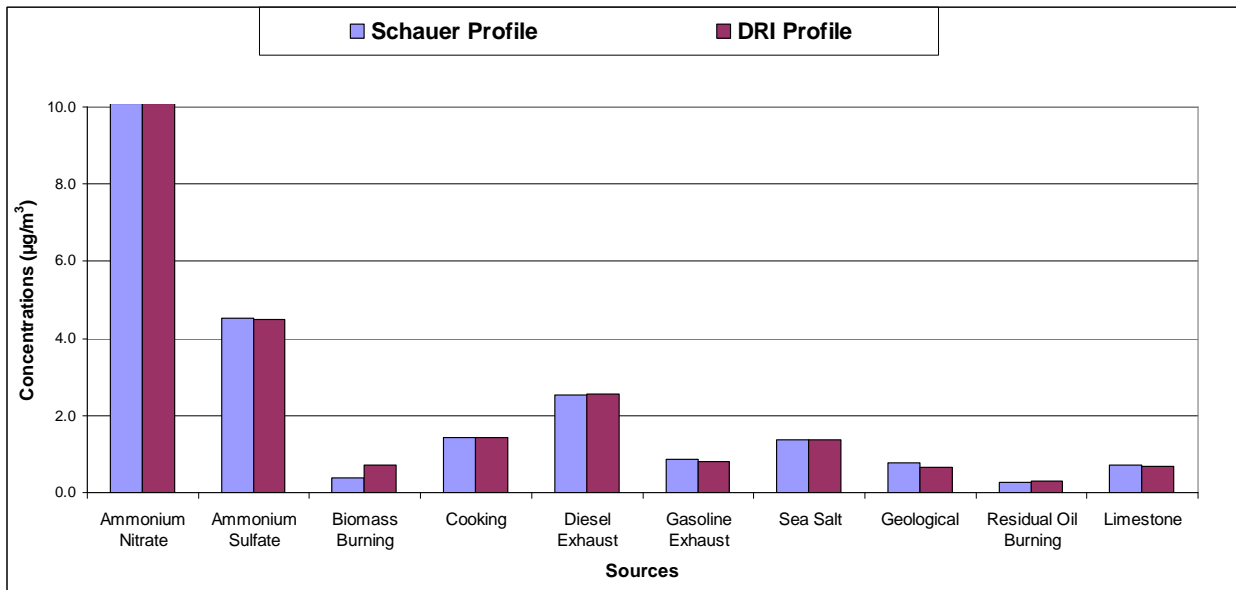


Figure VII-16. Rubidoux PM_{2.5} Source Contributions – Using Different Biomass Burning Profiles

VII-4 SUMMARY

Diesel is greater in the second year due to the higher second-year diesel exhaust contribution, which is driven by the higher EC ambient concentrations.

The use of different gasoline profiles slightly affects other source categories but has a large impact on gasoline contributions.

Gasoline exhaust contributions range from $0.60 \mu\text{g}/\text{m}^3$ to $1.75 \mu\text{g}/\text{m}^3$ for the first year and $0.73 \mu\text{g}/\text{m}^3$ to $1.75 \mu\text{g}/\text{m}^3$ for the second year, using the NFRAQS gasoline profile. The gasoline range varies from $0.16 \mu\text{g}/\text{m}^3$ to $0.51 \mu\text{g}/\text{m}^3$ for the first year and $0.16 \mu\text{g}/\text{m}^3$ to $0.45 \mu\text{g}/\text{m}^3$ for the second year, using the Basin gasoline profile. Based on the two-year site-averaged contributions, gasoline exhaust using the NFRAQS gasoline profile are approximately three to five times higher than those generated by the Basin profile. As a result, the average diesel-gasoline ratios range from 2.6 to 3.0 using the NFRAQS gasoline profile. These ratios become more significant (10.1 to 15.0) with the Basin gasoline profile, and are not supported by the 2007 AQMP diesel-gasoline ratio of 1.9 and Fujita, et al.'s (2006) ratio of 2.68. For that reason, the NFRAQS gasoline profile is the preferred profile for this CMB model.

The use of the DRI biomass burning profile also slightly affects other sources and results in biomass burning contributions that are approximately two times greater than the contributions using Schauer, et al.'s profile (1998). Based on the sensitivity tests, Schauer, et al.'s biomass burning profile is the preferred profile for the model.

VII-1. References

- Appel, B.R.; Wall, S.M.; Tokiwa, Y.; Haik, M., 1980. Simultaneous Nitric Acid, Particulate Nitrate and Acidity Measurements in Ambient Air, *Atmos. Environ.*, 14, 549-554.
- AQMD, 1989. AQMP – Final Appendix V-G - PM10 Source Profile Library for the South Coast Air Basin, 1989 AQMP.
- Chow, J.C., J.G. Watson, D.H. Lowenthal, L.W.A. Chen, B. Zielinska, L.R. Mazzoleni, and K.L. Magliano, 2007. Evaluation of Organic Markers for Chemical Mass Balance Source Apportionment at the Fresno Supersite, *Atmos. Chem. Phys.*, 7: 1741-1754.
- Chow, J.C., J.G. Watson, D.H. Lowenthal, and R.J. Countess, 1996. Sources and Chemistry of PM10 Aerosol in Santa Barbara County, CA, *Atmos. Environ.*, 30(9): 1489-1499.
- Chow, J.C., J.G. Watson, L.L. Ashbaugh, and K.L. Magliano, 2003. Similarities and Differences in PM10 Chemical Sources Profiles for Geological Dust from the San Joaquin Valley, California, *Atmos. Environ.*, 37(9-10): 1317-1340.
- Corbett, J.J. and P. Fischbeck, 1997. Emissions from Ships. *Science*, 278: 823-824.
- EPA, 2004. Protocol for Applying and Validating the CMB Model for PM2.5 and VOC. Report No. EPA-452/R-04-011. December 2004. Prepared by Watson, et al. for U.S. EPA, Research Triangle Park, NC.
- Fine, P.M., 2002. The Contribution of Biomass Combustion to Ambient Fine Particle Concentrations in the United States. Ph.D. Dissertation, California Institute of Technology, Pasadena, CA.
- Friedlander, S.K. 1973. Chemical Element Balances and Identification of Air Pollution Sources, *Environm. Sci. Technol.*, 7(3): 235-240.
- Fujita, E.M., B. Zielinska, D.E. Campbell, W.P. Arnott, J.C. Sagebiel, L. Reinhart, J.C. Chow, P.A. Gabele, W. Crews, R. Snow, N.N. Clark, W.S. Wayne, and D.R. Lawson, 2006. Variations in Speciated Emissions from Spark-Ignition and Compression-Ignition Motor Vehicles in California's South Coast Air Basin. Manuscript.
- Kim, B.M. and R.C. Henry, 1989. Analysis of Multicollinearity Indicators and Influential Species for Chemical Mass Balance Receptor Model. In *Transactions, Receptor Models in Air Resources Management*, J.G. Watson, Ed. J. Air & Waste Manage. Assoc., 379-390.
- Kim, B.M., S. Teffera, and M.D. Zeldin, 2000. Characterization of PM2.5 and PM10 in the South Coast Air Basin of Southern California: Part 1 – Spatial Variations, *J. Air & Waste Manage. Assoc.*, 50: 2034 – 2044.
- Lough, G.C., J.J. Schauer, D.R. Lawson, 2006. Day-of-week Trends in Carbonaceous Aerosol Composition in the Urban Atmosphere, *Atmospheric Environment*, 40: 4137-4149.

Lough, G.C., C.C. Chistensen, J.J. Schauer, J. Tortorelli, E. Bean, D.R. Lawson, N.N. Clark, P.A. Gabele. 2005. Development of Molecular Marker Source Profiles for Emissions from On-Road Gasoline and Diesel Vehicle Fleets, *J. Air & Waste Manage. Assoc.*, Submitted for Review.

Mathis, U., M. Mohr, and A.M. Forss, 2005. Comprehensive Particle Characterization of Modern Gasoline and Diesel Passenger Cars at Low Ambient Temperatures, *Atmos. Environ.*, 39(1): 107-117.

Miller, M.S., S.K. Friedlander, and G.M. Hidy, 1972. A Chemical Element Balance for the Pasadena Aerosol, *J. Colloid Interface Sci.*, 39: 165-176.

Russel, A.G.; McRae, G.J.; Cass, G.R., 1983. Mathematical Modeling of the Formation and Transport of Ammonium Nitrate Aerosol, *Atmos. Environ.*, 17, 949-964.

Schauer, J.J., 1998. Source Contributions to Atmospheric Organic Compound Concentrations: Emissions Measurements and Model Predictions. Ph.D. Dissertation, California Institute of Technology, Pasadena, CA.

Stelson, A.W.; Seinfeld, J.H., 1982. Relative Humidity and Temperature Dependence of the Ammonium Nitrate Dissociation Constant; *Atmos. Environ.*, 16, 983-992.

Turpin, B.J., J.J. Huntzicker, and S.V. Hering, 1994. Investigation of Organic Aerosol Sampling Artifacts in the Los Angeles Basin, *Atmos. Environ.*, 28(19): 3061-3071.

Watson, J.G., 1979. Chemical Element Balance Receptor Model Methodology for Assessing the Sources of Fine and Total Suspended Particulate Matter in Portland, Oregon. Ph.D. Dissertation, Oregon Graduate Center, Beaverton, OR.

Zielinska, B., J.D. McDonald, T. Hayes, J.C. Chow, E.M. Fujita, and J.G. Watson, 1998. Northern Front Range Air Quality Study. Volume B: Source Measurements. Prepared for Colorado State University, Fort Collins, CO.

Source Profiles Used for CMB Model

PNO	S21	S19	S14	RESWDBUR	DR1353	S08	S07	DR1387	S17	S01	S53	Portland
SID	AMNIT	AMSUL	BURN	SCHWDBUR	CHCHICK	DIES	GAS	GASO	Mar-50	PVRD	ResiOil3	CementKiln
SIZE	FINE	FINE	FINE	FINE	FINE	FINE	FINE	FINE	FINE	FINE	FINE	FINE
REF												
MSGC	1	1	1	1	1	1	1	1	1	1	1	1
MSGU	0.1	0.1	0.1	0.1	0.1	0.1	0.1	0.1	0.1	0.1	0.1	0.1
OCTC	0	0	0.583351	0.591	0.830617	0.416033	0.587718	0.663695	0	0.06895	0.032	0
OCTU	0	0	0.046528	0.03	0.060651	0.167461	0.215955	0.11833	0.001416	0.037295	0.005	0.0001
ECTC	0	0	0.051909	0.032	0.003231	0.525526	0.285649	0.184472	0	0.009946	0.077	0
ECTU	0	0	0.007901	0.002	0.002217	0.11106	0.138095	0.133081	0.001416	0.00952	0.015	0.0001
NAXC	0	0	0.003045	0.001	0.000829	0	0	0.00003	0.370809	0.000789	0.026	0
NAXU	0	0	0.000252	0.0001	0.001001	0.000007	0.00001	0.0011	0.042302	0.000351	0.006	0.0001
N4CC	0.2255	0.273	0.004565	0.001	0	0.007921	0.030173	0	0	0.003233	0.035	0
N4CU	0.02255	0.0273	0.003963	0.0001	0.0001	0.007969	0.031377	0.0001	0.001416	0.002305	0.016	0.0001
CLIC	0	0	0.014719	0.002	0	0.001591	0.004769	0	0.332596	0.001027	0.00018	0
CLIU	0	0	0.018146	0.0001	0.000704	0.002345	0.004318	0.01	0.037942	0.001839	0.00008	0.0001
N3IC	0.775	0	0.006803	0.0044	0	0.000907	0.016545	0.001251	0.00416	0.000435	0	0.0055
N3IU	0.0775	0	0.000567	0.0001	0.000772	0.002573	0.012115	0.000551	0.000475	0.001817	0.0001	0.00165
S4IC	0	0.727	0.014179	0.0041	0	0.024065	0.067749	0.002467	0.092703	0.002787	0.4	0.0427
S4IU	0	0.0727	0.006204	0.0001	0.000705	0.019995	0.069651	0.001449	0.010575	0.001881	0.03	0.01281
MGXC	0	0	0	0	0	0	0	0.000642	0	0	0	0
MGXU	0.0001	0.0001	0.0001	0.0001	0.000206	0.0001	0.0001	0.000484	0.0001	0.0001	0.0001	0.0001
ALXC	0	0	0.000944	0	0	0.001152	0.001073	0.00013	0	0.100008	0.0042	0
ALXU	0	0	0.000112	0.0001	0.000226	0.001151	0.000736	0.00025	0	0.030147	0.0008	0.0001
SIXC	0	0	0.002912	0.00016	0	0.008072	0.047878	0.003048	0.000103	0.281663	0.019	0
SIXU	0	0	0.00023	0.00005	0.000063	0.002447	0.041119	0.003189	1.13E-05	0.089603	0.006	0.0001
PHXC	0	0	0	0.00007	0	0.001196	0.003479	0	1.42E-06	0.003877	0.015	0
PHXU	0	0	0.000073	0.00002	0.0001	0.000372	0.005129	0.0001	0	0.003543	0.004	0.0001
SUXC	0	0.2427	0.00424	0.00148	0	0.009962	0.02667	0	0.030901	0.003516	0.11	0.024
SUXU	0	0.02427	0.000331	0.00004	0.0001	0.008032	0.024785	0.0001	0.003524	0.0021	0.02	0.004
CLXC	0	0	0.013544	0.00127	0	0.000515	0.002491	0	0.332596	0.001006	0	0
CLXU	0	0	0.015612	0.00006	0.0001	0.000285	0.002978	0.0001	0.037942	0.001422	0.0001	0.0001
KPXC	0	0	0.029511	0.00647	0	0.000735	0.000579	0.000021	0.013734	0.028206	0.0016	0.024
KPXU	0	0	0.006782	0.00007	0.000067	0.000611	0.000474	0.000114	0.001566	0.005488	0.0005	0.004
CAXC	0	0	0.001873	0.00008	0	0.004728	0.007865	0.001443	0.014146	0.03485	0.034	0.161
CAXU	0	0	0.000225	0.00011	0.000088	0.001892	0.014028	0.000554	0.001614	0.011771	0.009	0.03
SCXC	0	0	0	0	0	0	0	0	0	0	0	0
SCXU	0.0001	0.0001	0.0001	0.0001	0.0001	0.0001	0.0001	0.0001	0.0001	0.0001	0.0001	0.0001
TIXC	0	0	0.000129	0	0	0.000103	0.00003	0.000007	0	0.004553	0.0005	0.0055
TIXU	0	0	0.000197	0.00017	0.0006	0.000613	0.000569	0.000501	0	0.001348	0.0005	0.00165
VAXC	0	0	0	0	0	0	0	0.000004	0	0	0.011	0
VAXU	0.0001	0.0001	0.0001	0.00007	0.000244	0.0001	0.0001	0.000234	0.0001	0.0001	0.003	0.0001
CRXC	0	0	0	0	0	0	0	0.000011	0	0	0.00022	0
CRXU	0.0001	0.0001	0.0001	0.00002	0.00006	0.0001	0.0001	0.000079	0.0001	0.0001	0.00001	0.0001

Source Profiles Used for CMB Model

PNO	S21	S19	S14	RESWDBUR	DR1353	S08	S07	DR1387	S17	S01	S53	Portland
SID	AMNIT	AMSUL	BURN	SCHWDBUR	CHCHICK	DIES	GAS	GASO	Mar-50	PVRD	ResiOil3	CementKiln
SIZE	FINE	FINE	FINE	FINE	FINE	FINE	FINE	FINE	FINE	FINE	FINE	FINE
REF												
MNXC	0	0	0.000067	0	0	0.000009	0.000042	0.000008	0	0.000759	0.00035	0
MNXU	0	0	0.000007	0.00001	0.000045	0.000044	0.000042	0.000062	0	0.000054	0.00004	0.0001
FEXC	0	0	0.001402	0	0	0.004409	0.004226	0.000642	0	0.052254	0.015	0
FEXU	0	0	0.000114	0.00001	0.000017	0.002751	0.003424	0.000289	0	0.010428	0.002	0.0001
COXC	0	0	0	0	0	0	0	0	0	0	0.00075	0
COXU	0.0001	0.0001	0.0001	0.00001	0.0001	0.0001	0.0001	0.0001	0.0001	0.0001	0.00014	0.0001
NIXC	0	0	0	0	0	0	0	0.000004	0	0	0.015	0
NIXU	0.0001	0.0001	0.0001	0.00001	0.000031	0.0001	0.0001	0.000039	0.0001	0.0001	0.005	0.0001
CUXC	0	0	0.000067	0.00005	0	0.000105	0.000519	0.000191	0	0.000168	0.00098	0
CUXU	0	0	0.000006	0.00001	0.000017	0.000044	0.000537	0.000122	0	0.000119	0.00032	0.0001
ZNXC	0	0	0.001368	0.00005	0	0.002531	0.004335	0.001965	0	0.000965	0.012	0
ZNXU	0	0	0.000135	0.00001	0.000026	0.000585	0.004056	0.000988	0	0.000467	0.003	0.0001
GAXC	0	0	0	0	0	0	0	0	0	0	0	0
GAXU	0.0001	0.0001	0.0001	0.00002	0.0001	0.0001	0.0001	0.0001	0.0001	0.0001	0.0001	0.0001
GEXC	0	0	0	0	0	0	0	0	0	0	0	0
GEXU	0.0001	0.0001	0.0001	0.0001	0.0001	0.0001	0.0001	0.0001	0.0001	0.0001	0.0001	0.0001
ASXC	0	0	0.000007	0	0	0.000003	0.000001	0	0	0.000016	0.000031	0
ASXU	0	0	0.000017	0.00002	0.0001	0.000052	0.000052	0.0001	0	0.000027	0.000007	0.0001
SEXC	0	0	0.000001	0	0	0.000015	0.000002	0	0	0.000002	0.000022	0
SEXU	0	0	0.000007	0.00001	0.0001	0.000028	0.000027	0.0001	0	0.00001	0.000005	0.0001
RBXC	0	0	0.000046	0	0	0.000005	0.000005	0	0	0.000139	0	0
RBXU	0	0	0.000005	0.00001	0.0001	0.000026	0.000022	0.0001	0	0.000046	0.0001	0.0001
SRXC	0	0	0.000025	0	0	0.000019	0.000009	0	0.000272	0.000305	0.00016	0
SRXU	0	0	0.000004	0.00001	0.0001	0.000026	0.000023	0.0001	3.12E-05	0.000016	0.00005	0.0001
YTXC	0	0	0	0	0	0	0	0	0	0	0	0
YTXU	0.0001	0.0001	0.0001	0.00001	0.0001	0.0001	0.0001	0.0001	0.0001	0.0001	0.0001	0.0001
NBXC	0	0	0	0	0	0	0	0	0	0	0	0
NBXU	0.0001	0.0001	0.0001	0.0001	0.0001	0.0001	0.0001	0.0001	0.0001	0.0001	0.0001	0.0001
MOXC	0	0	0	0	0	0	0	0	0	0	0.00087	0
MOXU	0.0001	0.0001	0.0001	0.00002	0.0001	0.0001	0.0001	0.0001	0.0001	0.0001	0.00018	0.0001
PDXC	0	0	0	0	0	0	0	0	0	0	0	0
PDXU	0.0001	0.0001	0.0001	0.00006	0.0001	0.0001	0.0001	0.0001	0.0001	0.0001	0.0001	0.0001
AGXC	0	0	0	0	0	0	0	0	0	0	0	0
AGXU	0.0001	0.0001	0.0001	0.00007	0.0001	0.0001	0.0001	0.0001	0.0001	0.0001	0.0001	0.0001
CDXC	0	0	0	0	0	0	0	0	0	0	0	0
CDXU	0.0001	0.0001	0.0001	0.00007	0.0001	0.0001	0.0001	0.0001	0.0001	0.0001	0.0001	0.0001
INXC	0	0	0	0	0	0	0	0	0	0	0	0
INXU	0.0001	0.0001	0.0001	0.00008	0.0001	0.0001	0.0001	0.0001	0.0001	0.0001	0.0001	0.0001
SNXC	0	0	0	0.00001	0	0	0	0	0	0	0.00034	0
SNXU	0.0001	0.0001	0.0001	0.00011	0.0001	0.0001	0.0001	0.0001	0.0001	0.0001	0.00022	0.0001

Source Profiles Used for CMB Model

PNO	S21	S19	S14	RESWDBUR	DR1353	S08	S07	DR1387	S17	S01	S53	Portland
SID	AMNIT	AMSUL	BURN	SCHWDBUR	CHCHICK	DIES	GAS	GASO	Mar-50	PVRD	ResiOil3	CementKiln
SIZE	FINE	FINE	FINE	FINE	FINE	FINE	FINE	FINE	FINE	FINE	FINE	FINE
REF												
SBXC	0	0	0	0	0	0	0	0	0	0	0.00035	0
SBXU	0.0001	0.0001	0.0001	0.00013	0.0001	0.0001	0.0001	0.0001	0.0001	0.0001	0.00038	0.0001
CSXC	0	0	0	0	0	0	0	0	0	0	0	0
CSXU	0.0001	0.0001	0.0001	0.0001	0.0001	0.0001	0.0001	0.0001	0.0001	0.0001	0.0001	0.0001
BAXC	0	0	0	0	0	0	0	0	0	0	0.00186	0
BAXU	0.0001	0.0001	0.0001	0.00048	0.0001	0.0001	0.0001	0.0001	0.0001	0.0001	0.00009	0.0001
LAXC	0	0	0	0	0	0	0	0	0	0	0.00012	0
LAXU	0.0001	0.0001	0.0001	0.00065	0.0001	0.0001	0.0001	0.0001	0.0001	0.0001	0.00002	0.0001
PTXC	0	0	0	0	0	0	0	0	0	0	0	0
PTXU	0.0001	0.0001	0.0001	0.0001	0.0001	0.0001	0.0001	0.0001	0.0001	0.0001	0.0001	0.0001
AUXC	0	0	0	0	0	0	0	0	0	0	0	0
AUXU	0.0001	0.0001	0.0001	0.0001	0.0001	0.0001	0.0001	0.0001	0.0001	0.0001	0.0001	0.0001
PBXC	0	0	0.000039	0	0	0.000058	0.000257	0.000141	0	0.000109	0.018	0
PBXU	0	0	0.000009	0.00003	0.000084	0.00008	0.000241	0.000097	0	0.000074	0.006	0.0001
BIXC	0	0	0	0	0	0	0	0	0	0	0	0
BIXU	0.0001	0.0001	0.0001	0.0001	0.0001	0.0001	0.0001	0.0001	0.0001	0.0001	0.0001	0.0001
PYREN	0	0	0	0.000241	0.000304	0	0	0.001046	0	0	0	0
PYRENU	0.0001	0.0001	0.0001	0.0001	0.000111	0.0001	0.0001	0.000337	0.0001	0.0001	0.0001	0.0001
REten	0	0	0.000272	0.00022	4.22E-06	0.000001	0.000042	0	0	0	0	0
REtenU	0	0	0.000039	0.0001	3.71E-06	0.000006	0.000132	1.05E-05	0	0	0.0001	0.0001
BGHIF	0	0	0	8.22E-05	0	0	0	0	0	0	0	0
BGHIFU	0.0001	0.0001	0.0001	0.0001	0.0001	0.0001	0.0001	0.0001	0.0001	0.0001	0.0001	0.0001
BAANT	0	0	0	0	5.73E-05	0	0	0.000131	0	0	0	0
BAANTU	0.0001	0.0001	0.0001	0.0001	4.50E-05	0.0001	0.0001	5.34E-05	0.0001	0.0001	0.0001	0.0001
CHRYS	0	0	0	0	4.89E-05	0	0	0.000137	0	0	0	0
CHRYSU	0.0001	0.0001	0.0001	0.0001	1.20E-05	0.0001	0.0001	5.14E-05	0.0001	0.0001	0.0001	0.0001
BBJKF	0	0	0	0	4.02E-05	0	0	0.000167	0	0	0	0
BBJKFU	0.0001	0.0001	0.0001	0.0001	8.57E-06	0.0001	0.0001	9.49E-05	0.0001	0.0001	0.0001	0.0001
BEPYR	0	0	0	4.53E-05	9.99E-06	0	0	0.000125	0	0	0	0
BEPYRU	0.0001	0.0001	0.0001	0.0001	3.83E-06	0.0001	0.0001	8.41E-05	0.0001	0.0001	0.0001	0.0001
BAPYR	0	0	0	4.80E-05	1.67E-05	0	0	0.000178	0	0	0	0
BAPYRU	0.0001	0.0001	0.0001	0.0001	8.84E-06	0.0001	0.0001	0.000109	0.0001	0.0001	0.0001	0.0001
INDPY	0	0	0.000028	0	9.93E-06	0	0.00034	0.000102	0	0	0	0
INDPYU	0	0	0.000004	0.0001	7.21E-06	0.000009	0.000278	5.92E-05	0	0	0.0001	0.0001
DBANT	0	0	0	0	1.49E-06	0	0	9.43E-06	0	0	0	0
DBANTU	0.0001	0.0001	0.0001	0.0001	1.04E-05	0.0001	0.0001	2.93E-05	0.0001	0.0001	0.0001	0.0001
PIC	0	0	0	0	0	0	0	0	0	0	0	0
PICU	0.0001	0.0001	0.0001	0.0001	0.0001	0.0001	0.0001	0.0001	0.0001	0.0001	0.0001	0.0001
BGHIP	0	0	0.000029	0	1.45E-05	0	0.000941	0.000115	0	0	0	0
BGHIPU	0	0	0.000008	0.0001	9.42E-06	0.000011	0.000827	0.000196	0	0	0.0001	0.0001

Source Profiles Used for CMB Model

PNO	S21	S19	S14	RESWDBUR	DR1353	S08	S07	DR1387	S17	S01	S53	Portland
SID	AMNIT	AMSUL	BURN	SCHWDBUR	CHCHICK	DIES	GAS	GASO	Mar-50	PVRD	ResiOil3	CementKiln
SIZE	FINE	FINE	FINE	FINE	FINE	FINE	FINE	FINE	FINE	FINE	FINE	FINE
REF												
CORON	0	0	0.000011	0	8.57E-06	0	0.000836	0.000133	0	0	0	0
CORONU	0	0	0.000003	0.0001	1.87E-05	0.000003	0.00092	0.000121	0	0	0.0001	0.0001
STR42	0	0	0	0	0	0	0	0	0	0	0	0
STR42U	0.0001	0.0001	0.0001	0.0001	0.0001	0.0001	0.0001	0.0001	0.0001	0.0001	0.0001	0.0001
STR43	0	0	0	0	2.75E-05	0	0	9.33E-05	0	0	0	0
STR43U	0.0001	0.0001	0.0001	0.0001	2.75E-05	0.0001	0.0001	9.33E-05	0.0001	0.0001	0.0001	0.0001
STR44	0	0	0	0	3.32E-05	0	0	2.93E-05	0	0	0	0
STR44U	0.0001	0.0001	0.0001	0.0001	2.29E-05	0.0001	0.0001	9.92E-06	0.0001	0.0001	0.0001	0.0001
ST454	0	0	0	0	0	0	0	0	0	0	0	0
ST454U	0.0001	0.0001	0.0001	0.0001	0.0001	0.0001	0.0001	0.0001	0.0001	0.0001	0.0001	0.0001
STR46	0	0	0	0	0	0	0	0	0	0	0	0
STR46U	0.0001	0.0001	0.0001	0.0001	0.0001	0.0001	0.0001	0.0001	0.0001	0.0001	0.0001	0.0001
STR47	0	0	0	0	0	0	0	0	0	0	0	0
STR47U	0.0001	0.0001	0.0001	0.0001	0.0001	0.0001	0.0001	0.0001	0.0001	0.0001	0.0001	0.0001
STR48	0	0	0	0	0	0	0.000031	0.000117	0	0	0	0
STR48U	0	0	0.000001	0.0001	0.0001	0.000006	0.000037	4.24E-05	0	0	0.0001	0.0001
STR49	0	0	0	0	0	0.000007	0.000431	0	0	0	0	0
STR49U	0	0	0.000001	0.0001	0.0001	0.000018	0.000978	0.0001	0	0	0.0001	0.0001
STR50	0	0	0	0	0	0	0	0	0	0	0	0
STR50U	0.0001	0.0001	0.0001	0.0001	0.0001	0.0001	0.0001	0.0001	0.0001	0.0001	0.0001	0.0001
STR51	0	0	0	0	0	0	0	0	0	0	0	0
STR51U	0.0001	0.0001	0.0001	0.0001	0.0001	0.0001	0.0001	0.0001	0.0001	0.0001	0.0001	0.0001
STR52	0	0	0	0	1.04E-05	0	0	0	0	0	0	0
STR52U	0.0001	0.0001	0.0001	0.0001	7.64E-06	0.0001	0.0001	7.53E-06	0.0001	0.0001	0.0001	0.0001
HOP13	0	0	0	0	0	0	0	0	0	0	0	0
HOP13U	0.0001	0.0001	0.0001	0.0001	0.0001	0.0001	0.0001	0.0001	0.0001	0.0001	0.0001	0.0001
STR53	0	0	0	0	0.000457	0	0	0	0	0	0	0
STR53U	0.0001	0.0001	0.0001	0.0001	0.000585	0.0001	0.0001	7.53E-06	0.0001	0.0001	0.0001	0.0001
HOP15	0	0	0	0	2.09E-05	0	0	2.44E-05	0	0	0	0
HOP15U	0.0001	0.0001	0.0001	0.0001	2.74E-05	0.0001	0.0001	1.78E-05	0.0001	0.0001	0.0001	0.0001
HOP17	0	0	0.000001	0	0	0.000079	0.000146	0.00014	0	0	0	0
HOP17U	0	0	0.000002	0.0001	0.0001	0.00005	0.000262	0.000107	0	0	0.0001	0.0001
HOP19	0	0	0.000006	0	1.34E-05	0.000042	0.000446	9.12E-05	0	0	0	0
HOP19U	0	0	0.000002	0.0001	1.18E-05	0.000031	0.000791	6.25E-05	0	0	0.0001	0.0001
HOP20	0	0	0	0	0	0	0	9.95E-06	0	0	0	0
HOP20U	0.0001	0.0001	0.0001	0.0001	0.0001	0.0001	0.0001	1.22E-05	0.0001	0.0001	0.0001	0.0001
HOP21	0	0	0	0	0	0	0	4.50E-05	0	0	0	0
HOP21U	0.0001	0.0001	0.0001	0.0001	0.0001	0.0001	0.0001	3.00E-05	0.0001	0.0001	0.0001	0.0001
HOP22	0	0	0	0	0	0	0	3.33E-05	0	0	0	0
HOP22U	0.0001	0.0001	0.0001	0.0001	0.0001	0.0001	0.0001	2.20E-05	0.0001	0.0001	0.0001	0.0001

Source Profiles Used for CMB Model

PNO	S21	S19	S14	RESWDBUR	DR1353	S08	S07	DR1387	S17	S01	S53	Portland
SID	AMNIT	AMSUL	BURN	SCHWDBUR	CHCHICK	DIES	GAS	GASO	Mar-50	PVRD	ResiOil3	CementKiln
SIZE	FINE	FINE	FINE	FINE	FINE	FINE	FINE	FINE	FINE	FINE	FINE	FINE
REF												
HOP23	0	0	0	0	0	0	0	2.52E-05	0	0	0	0
HOP23U	0.0001	0.0001	0.0001	0.0001	0.0001	0.0001	0.0001	1.75E-05	0.0001	0.0001	0.0001	0.0001
HOP24	0	0	0.000005	0	0	0	0.000026	1.95E-05	0	0	0	0
HOP24U	0	0	0.000003	0.0001	0.002665	0.000006	0.000054	1.02E-05	0	0	0.0001	0.0001
HOP25	0	0	0	0	0	0	0	0	0	0	0	0
HOP25U	0.0001	0.0001	0.0001	0.0001	0.0001	0.0001	0.0001	0.0001	0.0001	0.0001	0.0001	0.0001
HOP26	0	0	0.000001	0	0	0	0.000025	0	0	0	0	0
HOP26U	0	0	0.000002	0.0001	0.0001	0.000006	0.000052	0.0001	0	0	0.0001	0.0001
HOP27	0	0	0	0	0	0	0	0	0	0	0	0
HOP27U	0.0001	0.0001	0.0001	0.0001	0.0001	0.0001	0.0001	0.0001	0.0001	0.0001	0.0001	0.0001
GUAI	0	0	0.003721	2.92E-05	0	0	0	0	0	0	0	0
GUAIU	0	0	0.000309	0.0001	0.0001	0	0	0.0001	0	0	0.0001	0.0001
SUCAC	0	0	0	0	0	0	0	0	0	0	0	0
SUCACU	0.0001	0.0001	0.0001	0.0001	0.0001	0.0001	0.0001	0.0001	0.0001	0.0001	0.0001	0.0001
SYRI	0	0	0	0.00039	0.000164	0	0	8.84E-06	0	0	0	0
SYRIU	0.0001	0.0001	0.0001	0.0001	0.000179	0.0001	0.0001	1.53E-05	0.0001	0.0001	0.0001	0.0001
GUAC	0	0	0	0	0	0	0	0	0	0	0	0
GUACU	0.0001	0.0001	0.0001	0.0001	0.0001	0.0001	0.0001	0.0001	0.0001	0.0001	0.0001	0.0001
HEXDA	0	0	0	0	0	0	0	0	0	0	0	0
HEXDAU	0.0001	0.0001	0.0001	0.0001	0.0001	0.0001	0.0001	0.0001	0.0001	0.0001	0.0001	0.0001
CPINA	0	0	0	0	0	0	0	0	0	0	0	0
CPINAU	0.0001	0.0001	0.0001	0.0001	0.0001	0.0001	0.0001	0.0001	0.0001	0.0001	0.0001	0.0001
FGUA4	0	0	0	0	0.000221	0	0	5.66E-07	0	0	0	0
FGUA4U	0.0001	0.0001	0.0001	0.0001	3.69E-05	0.0001	0.0001	7.53E-06	0.0001	0.0001	0.0001	0.0001
PHTHA	0	0	0.000141	0	0	0.001251	0.001026	0	0	0	0	0
PHTHAU	0	0	0.00001	0.0001	0.0001	0.001168	0.002018	0.0001	0	0	0.0001	0.0001
LEVG	0	0	0.022778	0.138431	0	0	0	0	0	0	0	0
LEVGU	0	0	0.005924	0.0001	0.0001	0.000117	0.00012	0.0001	0	0	0.0001	0.0001
SYRAL	0	0	0.004631	0.004961	9.73E-05	0	0	7.16E-05	0	0	0	0
SYRALU	0	0	0.000307	0.0001	7.82E-05	0	0	0.000117	0	0	0.0001	0.0001
ISPHA	0	0	0	0	0	0	0	0	0	0	0	0
ISPHAU	0.0001	0.0001	0.0001	0.0001	0.0001	0.0001	0.0001	0.0001	0.0001	0.0001	0.0001	0.0001
AZEAC	0	0	0	0	0	0	0	0	0	0	0	0
AZEACU	0.0001	0.0001	0.0001	0.0001	0.0001	0.0001	0.0001	0.0001	0.0001	0.0001	0.0001	0.0001
PALOL	0	0	0.000069	0	0	0.000176	0.000082	0	0	0	0	0
PALOLU	0	0	0.000005	0.0001	0.0001	0.000146	0.000117	0.0001	0	0	0.0001	0.0001
PALAC	0	0	0.000562	0.003314	0	0	0	0	0	0	0	0
PALACU	0	0	0.000041	0	0.0001	0.001011	0.000486	0.0001	0	0	0.0001	0.0001
OLAC	0	0	0.000652	0.002294	0	0	0	0	0	0	0	0
OLACU	0	0	0.000051	0	0.0001	0.000283	0.000152	0.0001	0	0	0.0001	0.0001

Source Profiles Used for CMB Model

PNO	S21	S19	S14	RESWDBUR	DR1353	S08	S07	DR1387	S17	S01	S53	Portland
SID	AMNIT	AMSUL	BURN	SCHWDBUR	CHCHICK	DIES	GAS	GASO	Mar-50	PVRD	ResiOil3	CementKiln
SIZE	FINE	FINE	FINE	FINE	FINE	FINE	FINE	FINE	FINE	FINE	FINE	FINE
REF												
STEAC	0	0	0.000174	0.000543	0	0	0	0	0	0	0	0
STEACU	0	0	0.000013	0	0.0001	0.00024	0.000173	0.0001	0	0	0.0001	0.0001
ISOPI	0	0	0	0.000696	0	0	0	0	0	0	0	0
ISOPIU	0.0001	0.0001	0.0001	0	0.0001	0.0001	0.0001	0.0001	0.0001	0.0001	0.0001	0.0001
DHABA	0	0	0	0.000406	0	0	0	0	0	0	0	0
DHABAU	0.0001	0.0001	0.0001	0	0.0001	0.0001	0.0001	0.0001	0.0001	0.0001	0.0001	0.0001
ABAC	0	0	0	0.000235	0	0	0	0	0	0	0	0
ABACU	0.0001	0.0001	0.0001	0.0001	0.0001	0.0001	0.0001	0.0001	0.0001	0.0001	0.0001	0.0001
OXDH7	0	0	0	0	0	0	0	0	0	0	0	0
OXDH7U	0.0001	0.0001	0.0001	0.0001	0.0001	0.0001	0.0001	0.0001	0.0001	0.0001	0.0001	0.0001
CHOL	0	0	0	0	0.001331	0	0	0	0	0	0	0
CHOLU	0	0	0	0.0001	0.000576	0.000013	0.000011	7.53E-06	0	0	0.0001	0.0001
PHYTA	0	0	0.000015	0	0	0.000654	0.000139	0	0	0	0	0
PHYTAU	0	0	0.000005	0.0001	0.0001	0.00044	0.004463	0.0001	0	0	0.0001	0.0001
DOCOS	0	0	0	0	0	0	0	0	0	0	0	0
DOCOSU	0.0001	0.0001	0.0001	0.0001	0.0001	0.0001	0.0001	0.0001	0.0001	0.0001	0.0001	0.0001
DC6YH	0	0	0	0	0	0	0	0	0	0	0	0
DC6YHU	0.0001	0.0001	0.0001	0.0001	0.0001	0.0001	0.0001	0.0001	0.0001	0.0001	0.0001	0.0001
TRICO	0	0	0	0	0	0	0	0	0	0	0	0
TRICOU	0.0001	0.0001	0.0001	0.0001	0.0001	0.0001	0.0001	0.0001	0.0001	0.0001	0.0001	0.0001
DC7YH	0	0	0	0	0	0	0	0	0	0	0	0
DC7YHU	0.0001	0.0001	0.0001	0.0001	0.0001	0.0001	0.0001	0.0001	0.0001	0.0001	0.0001	0.0001
DC8YH	0	0	0	0	0	0	0	0	0	0	0	0
DC8YHU	0.0001	0.0001	0.0001	0.0001	0.0001	0.0001	0.0001	0.0001	0.0001	0.0001	0.0001	0.0001
TETCO	0	0	0	0	0	0	0	0	0	0	0	0
TETCOU	0.0001	0.0001	0.0001	0.0001	0.0001	0.0001	0.0001	0.0001	0.0001	0.0001	0.0001	0.0001
PENCO	0	0	0	0	0	0	0	0	0	0	0	0
PENCOU	0.0001	0.0001	0.0001	0.0001	0.0001	0.0001	0.0001	0.0001	0.0001	0.0001	0.0001	0.0001
DC9YH	0	0	0	0	0	0	0	0	0	0	0	0
DC9YHU	0.0001	0.0001	0.0001	0.0001	0.0001	0.0001	0.0001	0.0001	0.0001	0.0001	0.0001	0.0001
HEXCO	0	0	0	6.47E-05	0	0	0	0	0	0	0	0
HEXCOU	0.0001	0.0001	0.0001	0.0001	0.0001	0.0001	0.0001	0.0001	0.0001	0.0001	0.0001	0.0001
CYHXE	0	0	0	0	0	0	0	0	0	0	0	0
CYHXEU	0.0001	0.0001	0.0001	0.0001	0.0001	0.0001	0.0001	0.0001	0.0001	0.0001	0.0001	0.0001
HEPCO	0	0	0	3.98E-05	0	0	0	0	0	0	0	0
HEPCOU	0.0001	0.0001	0.0001	0.0001	0.0001	0.0001	0.0001	0.0001	0.0001	0.0001	0.0001	0.0001
CYHHE	0	0	0	0	0	0	0	0	0	0	0	0
CYHHEU	0.0001	0.0001	0.0001	0.0001	0.0001	0.0001	0.0001	0.0001	0.0001	0.0001	0.0001	0.0001
OCTCO	0	0	0	1.33E-05	0	0	0	0	0	0	0	0
OCTCOU	0.0001	0.0001	0.0001	0.0001	0.0001	0.0001	0.0001	0.0001	0.0001	0.0001	0.0001	0.0001

Source Profiles Used for CMB Model

PNO	S21	S19	S14	RESWDBUR	DR1353	S08	S07	DR1387	S17	S01	S53	Portland
SID	AMNIT	AMSUL	BURN	SCHWDBUR	CHCHICK	DIES	GAS	GASO	Mar-50	PVRD	ResiOil3	CementKiln
SIZE	FINE	FINE	FINE	FINE	FINE	FINE	FINE	FINE	FINE	FINE	FINE	FINE
REF												
NONCO	0	0	0	4.53E-05	0	0	0	0	0	0	0	0
NONCOU	0.0001	0.0001	0.0001	0.0001	0.0001	0.0001	0.0001	0.0001	0.0001	0.0001	0.0001	0.0001
HTRIC	0	0	0	0	0	0	0	0	0	0	0	0
HTRICU	0.0001	0.0001	0.0001	0.0001	0.0001	0.0001	0.0001	0.0001	0.0001	0.0001	0.0001	0.0001
TTRIC	0	0	0	0	0	0	0	0	0	0	0	0
TTRICU	0.0001	0.0001	0.0001	0.0001	0.0001	0.0001	0.0001	0.0001	0.0001	0.0001	0.0001	0.0001

PNO: Profile name

SID: Source.

Source Profile Species Codes	
Code	Description
ABAC	abietic acid
ABACU	abietic acid uncertainty
AGXC	Silver concentration
AGXU	Silver concentration uncertainty
ALXC	Aluminum concentration
ALXU	Aluminum concentration uncertainty
ASXC	Arsenic concentration
ASXU	Arsenic concentration uncertainty
AUXC	Gold concentration
AUXU	Gold concentration uncertainty
AZEAC	azelaic acid (d-c9)
AZEACU	azelaic acid (d-c9) uncertainty
BAANT	Benz(a)anthracene
BAANTU	Benz(a)anthracene uncertainty
BAPYR	Benzo(a)Pyrene
BAPYRU	Benzo(a)Pyrene uncertainty
BAXC	Barium concentration
BAXU	Barium concentration uncertainty
BBJKF	Benzo(b+j+k)fluoranthene
BBJKFU	Benzo(b+j+k)fluoranthene uncertainty
BEPYR	Benzo(e)Pyrene
BEPYRU	Benzo(e)Pyrene uncertainty
BGHIF	Benzo(ghi)fluoranthene
BGHIFU	Benzo(ghi)fluoranthene concentration uncertainty
BGHIP	Benzo(ghi)perylene
BGHIPU	Benzo(ghi)perylene uncertainty
BIXC	Bismuth
BIXU	Bismuth concentration uncertainty
CAXC	Calcium concentration
CAXU	Calcium concentration uncertainty
CDXC	Cadmium concentration
CDXU	Cadmium concentration uncertainty
CHOL	cholesterol
CHOLU	cholesterol uncertainty
CHRYS	Chrysene
CHRYSU	Chrysene uncertainty
CLIC	Chloride concentration
CLIU	Chloride concentration uncertainty
CLXC	Chlorine concentration
CLXU	Chlorine concentration uncertainty
CORON	Coronene
CORONU	Coronene uncertainty
COXC	Cobalt concentration
COXU	Cobalt concentration uncertainty
CPINA	cis-pinonic acid
CPINAU	cis-pinonic acid concentration uncertainty

Source Profile Species Codes	
Code	Description
CRXC	Chromium concentration
CRXU	Chromium concentration uncertainty
CSXC	Cesium
CUXC	Copper concentration
CUXU	Copper concentration uncertainty
CYHHE	Heneicosylcyclohexane
CYHHEU	Heneicosylcyclohexane concentration uncertainty
CYHXE	Eicosylcyclohexane
CYHXEU	Eicosylcyclohexane concentration uncertainty
DBANT	Dibenzo(ah+ac)anthracene
DBANTU	Dibenzo(ah+ac)anthracene uncertainty
DC6YH	Hexadecylcyclohexane
DC6YHU	Hexadecylcyclohexane uncertainty
DC7YH	Heptadecylcyclohexane
DC7YHU	Heptadecylcyclohexane uncertainty
DC8YH	Octadecylcyclohexane
DC8YHU	Octadecylcyclohexane uncertainty
DC9YH	Nonadecylcyclohexane
DC9YHU	Nonadecylcyclohexane uncertainty
DHABA	dehydroabiatic acid
DHABAU	dehydroabiatic acid uncertainty
DOCOS	Docosane
DOCOSU	Docosane uncertainty
ECTC	Elemental Carbon concentration
ECTU	Elemental Carbon concentration uncertainty
FEXC	Iron concentration
FEXU	Iron concentration uncertainty
FGUA4	4-formyl-guaiacol (vanillin)
FGUA4U	4-formyl-guaiacol (vanillin) concentration uncertainty
GAXC	Gallium concentration
GAXU	Gallium concentration uncertainty
GEXC	Germanium
GUAC	glutaric acid (d-c5)
GUACU	glutaric acid (d-c5) concentration uncertainty
GUAI	guaiacol
GUAIU	guaiacol uncertainty
HEPCO	Heptacosane
HEPCOU	Heptacosane concentration uncertainty
HEXCO	Hexacosane
HEXCOU	Hexacosane concentration uncertainty
HEXDA	hexanedioic (adipic) acid (d-c6)
HEXDAU	hexanedioic (adipic) acid (d-c6) uncertainty
HOP13	18a(H),21β(H)-22,29,30-Trisnorhopane
HOP13U	18a(H),21β(H)-22,29,30-Trisnorhopane uncertainty
HOP15	17a(H),21β(H)-22,29,30-Trisnorhopane
HOP15U	17a(H),21β(H)-22,29,30-Trisnorhopane uncertainty

Source Profile Species Codes	
Code	Description
HOP17	17a(H),21β(H)-30-Norhopane
HOP17U	17a(H),21β(H)-30-Norhopane uncertainty
HOP19	17a(H),21β(H)-Hopane
HOP19U	17a(H),21β(H)-Hopane uncertainty
HOP20	17β(H),21a(H)-hopane
HOP20U	17β(H),21a(H)-hopane uncertainty
HOP21	22S-17a(H),21β(H)-30-Homohopane
HOP21U	22S-17a(H),21β(H)-30-Homohopane uncertainty
HOP22	22R-17a(H),21β(H)-30-Homohopane
HOP22U	22R-17a(H),21β(H)-30-Homohopane uncertainty
HOP23	17β(H),21β(H)-Hopane
HOP23U	17β(H),21β(H)-Hopane uncertainty
HOP24	22S-17a(H),21β(H)-30,31-Bishomohopane
HOP24U	22S-17a(H),21β(H)-30,31-Bishomohopane uncertainty
HOP25	22R-17a(H),21β(H)-30,31-Bishomohopane
HOP25U	22R-17a(H),21β(H)-30,31-Bishomohopane uncertainty
HOP26	22S-17a(H),21β(H)-30,31,32-Trisomohopane
HOP26U	22S-17a(H),21β(H)-30,31,32-Trisomohopane uncertainty
HOP27	22R-17a(H),21β(H)-30,31,32-Trishomohopane
HOP27U	22R-17a(H),21β(H)-30,31,32-Trishomohopane uncertainty
HTRIC	Hentriacontane
HTRICU	Hentriacontane concentration uncertainty
INDPY	Indeno[123-cd]pyrene
INDPYU	Indeno[123-cd]pyrene uncertainty
INXC	Indium concentration
INXU	Indium concentration uncertainty
ISOPI	isopimaric acid
ISOPIU	isopimaric acid concentration uncertainty
ISPHA	isophthalic acid
ISPHAU	isophthalic acid concentration uncertainty
KPXC	Potassium concentration
KPXU	Potassium concentration uncertainty
LAXC	Lanthanum concentration
LAXU	Lanthanum concentration uncertainty
LEVG	levoglucosan
LEVGU	levoglucosan uncertainty
MGXC	Magnesium concentration (qualitative only)
MGXU	Magnesium concentration uncertainty
MNXC	Manganese concentration
MNXU	Manganese concentration uncertainty
MOXC	Molybdenum concentration
MOXU	Molybdenum concentration uncertainty
MSGC	Mass concentration
MSGU	Mass concentration uncertainty
N3IC	Nitrate concentration
N3IU	Nitrate concentration uncertainty

Source Profile Species Codes	
Code	Description
N4CC	Ammonium concentration
N4CU	Ammonium concentration uncertainty
NAXC	Sodium concentration (qualitative only)
NAXU	Sodium concentration uncertainty
NBXC	Niobium
NIXC	Nickel concentration
NIXU	Nickel concentration uncertainty
NONCO	Nonacosane
NONCOU	Nonacosane concentration uncertainty
OCTC	Organic Carbon concentration
OCTCO	Octacosane
OCTCOU	Octacosane concentration uncertainty
OCTU	Organic Carbon concentration uncertainty
OLAC	oleic acid
OLACU	oleic acid uncertainty
OXDH7	7-oxodehydroabietic acid
OXDH7U	7-oxodehydroabietic acid concentration uncertainty
PALAC	palmitic acid (c16)
PALACU	palmitic acid (c16) uncertainty
PALOL	palmitoleic acid
PALOLU	palmitoleic acid concentration uncertainty
PBXC	Lead concentration
PBXU	Lead concentration uncertainty
PDXC	Palladium concentration
PDXU	Palladium concentration uncertainty
PENCO	Pentacosane
PENCOU	Pentacosane concentration uncertainty
PHTHA	phthalic acid
PHTHAU	phthalic acid uncertainty
PHXC	Phosphorous concentration
PHXU	Phosphorous concentration uncertainty
PHYTA	Phytane
PHYTAU	Phytane uncertainty
PIC	picolinic acid
PICU	picolinic acid uncertainty
PTXC	Platinum
PYREN	Pyrene
PYRENU	Pyrene uncertainty
RBXC	Rubidium concentration
RBXU	Rubidium concentration uncertainty
RETEN	Retene
RETENU	Retene uncertainty
S4IC	Sulfate concentration
S4IU	Sulfate concentration uncertainty
SBXC	Antimony concentration
SBXU	Antimony concentration uncertainty

Source Profile Species Codes	
Code	Description
SCXC	Scandium
SEXC	Selenium concentration
SEXU	Selenium concentration uncertainty
SIXC	Silicon concentration
SIXU	Silicon concentration uncertainty
SNXC	Tin concentration
SNXU	Tin concentration uncertainty
SRXC	Strontium concentration
SRXU	Strontium concentration uncertainty
ST454	C27-20R5a(H),14a(H),17a(H)-cholestane&C29-20S13β(H),17a(H)-diasterane
ST454U	C27-20R5a(H),14a(H),17a(H)-cholestane&C29-20S13β(H),17a(H)-diasterane uncertainty
STEAC	stearic acid (c18)
STEACU	stearic acid (c18) uncertainty
STR42	C27-20S5a(H),14a(H)-cholestane
STR42U	C27-20S5a(H),14a(H)-cholestane uncertainty
STR43	C27-20R5a(H),14β(H)-cholestane
STR43U	C27-20R5a(H),14β(H)-cholestane uncertainty
STR44	C27-20S5a(H),14β(H),17β(H)-cholestane
STR44U	C27-20S5a(H),14β(H),17β(H)-cholestane uncertainty
STR46	C28-20S5a(H),14a(H),17a(H)-ergostane
STR46U	C28-20S5a(H),14a(H),17a(H)-ergostane uncertainty
STR47	C28-20R5a(H),14β(H),17β(H)-ergostane
STR47U	C28-20R5a(H),14β(H),17β(H)-ergostane uncertainty
STR48	C28-20S5a(H),14β(H),17β(H)-ergostane
STR48U	C28-20S5a(H),14β(H),17β(H)-ergostane uncertainty
STR49	C28-20R5a(H),14a(H),17a(H)-ergostane
STR49U	C28-20R5a(H),14a(H),17a(H)-ergostane uncertainty
STR50	C29-20S5a(H),14a(H),17a(H)-stigmastane
STR50U	C29-20S5a(H),14a(H),17a(H)-stigmastane uncertainty
STR51	C29-20R5a(H),14β(H),17β(H)-stigmastane
STR51U	C29-20R5a(H),14β(H),17β(H)-stigmastane uncertainty
STR52	C29-20S5a(H),14β(H),17β(H)-stigmastane
STR52U	C29-20S5a(H),14β(H),17β(H)-stigmastane uncertainty
STR53	C29-20R5a(H),14a(H),17a(H)-stigmastane
STR53U	C29-20R5a(H),14a(H),17a(H)-stigmastane uncertainty
SUCAC	succinic acid (d-c4)
SUCACU	succinic acid (d-c4) uncertainty
SUXC	Sulfur concentration
SUXU	Sulfur concentration uncertainty
SYRAL	syringaldehyde
SYRALU	syringaldehyde concentration uncertainty
SYRI	syringol
SYRIU	syringol uncertainty
TETCO	Tetracosane
TETCOU	Tetracosane concentration uncertainty
TIXC	Titanium concentration

Source Profile Species Codes	
Code	Description
TIXU	Titanium concentration uncertainty
TRICO	Tricosane
TRICOU	Tricosane uncertainty
TTRIC	Tritriacontane
TTRICU	Tritriacontane concentration uncertainty
VAXC	Vanadium concentration
VAXU	Vanadium concentration uncertainty
YTXC	Yttrium concentration
YTXU	Yttrium concentration uncertainty
ZNXC	Zinc concentration
ZNXU	Zinc concentration uncertainty